

Review

# Magnetic Micro and Nano Sensors for Continuous Health Monitoring

Tomasz Blachowicz <sup>1</sup>, Ilda Kola <sup>2</sup>, Andrea Ehrmann <sup>3</sup>, Karoline Guenther <sup>4</sup> and Guido Ehrmann <sup>5,\*</sup>

<sup>1</sup> Institute of Physics—Center for Science and Education, Silesian University of Technology, 44-100 Gliwice, Poland; tomasz.blachowicz@polsl.pl

<sup>2</sup> Department of Textile and Fashion, Polytechnic University of Tirana, 1019 Tirana, Albania; ikola@fim.edu.al

<sup>3</sup> Institute for Technical Energy Systems (ITES), Faculty of Engineering Sciences and Mathematics, Bielefeld University of Applied Sciences and Arts, 33619 Bielefeld, Germany; andrea.ehrmann@hsbi.de

<sup>4</sup> Saurer Spinning Solutions GmbH & Co. KG, Carlstraße 60, 52531 Übach-Palenberg, Germany; karoline.guenther@saurer.com

<sup>5</sup> Virtual Institute of Applied Research on Advanced Materials (VIARAM)

\* Correspondence: guido.ehrmann@gmx.de

**Abstract:** Magnetic micro and nano sensors can be used in a broad variety of applications, e.g., for navigation, automobiles, smartphones and also for health monitoring. Based on physical effects such as the well-known magnetic induction, the Hall effect, tunnel magnetoresistance and giant magnetoresistance, they can be used to measure positions, flow, pressure and other physical properties. In biomedicine and healthcare, these miniaturized sensors can be either integrated into garments and other wearables, be directed through the body by passive capsules or active micro-robots or be implanted, which usually necessitates bio-functionalization and avoiding cell-toxic materials. This review describes the physical effects that can be applied in these sensors and discusses the most recent micro and nano sensors developed for healthcare applications.

**Keywords:** Hall effect; giant magnetoresistance; tunnel magnetoresistance; anisotropic magnetoresistance; giant magnetoimpedance



**Citation:** Blachowicz, T.; Kola, I.; Ehrmann, A.; Guenther, K.; Ehrmann, G. Magnetic Micro and Nano Sensors for Continuous Health Monitoring. *Micro* **2024**, *4*, 206–228. <https://doi.org/10.3390/micro4020015>

Received: 28 February 2024

Revised: 20 March 2024

Accepted: 3 April 2024

Published: 6 April 2024



**Copyright:** © 2024 by the authors. Licensee MDPI, Basel, Switzerland. This article is an open access article distributed under the terms and conditions of the Creative Commons Attribution (CC BY) license (<https://creativecommons.org/licenses/by/4.0/>).

## 1. Introduction

Monitoring the health of patients, the elderly and athletes becomes more and more important with the increased number of sensor systems available, on the one hand, and an increasing number of elderly people, on the other hand [1]. Wearable systems are preferred for long-term monitoring during active aging, as well as in sports [2,3].

Wearable sensors can measure diverse vital parameters using a broad variety of different physical principles [4]. Amongst the most often measured parameters are heart rate and ECG, blood oxygen saturation, blood pressure, sleep patterns and physical activities, which are measured by bioelectric, mechano-electric, opto-electric or ultrasonic sensors [5–7]. Alternatively, optical sensors enable the measuring of temperature, light, pH or electric fields [8]. However, there are many more sensors which are typically used in wearables, such as skin temperature sensors, pedometers, GPS (geographical positioning system), accelerometers or EMG (electromyography) sensors [9,10]. Besides these body functions, wearable sensors can also detect environmental stimuli, such as light, temperature, magnetic field or volatile organic compounds (VOCs) [11]. It should be mentioned that these sensors alone are not sufficient to monitor a person's health, and that data evaluation either by a medical doctor or supported by automatic procedures, e.g., based on deep learning and artificial intelligence, is necessary to detect chronic diseases as well as sudden health problems as soon as possible [12,13]. This review, however, focuses on the sensors used for continuous health monitoring.

One of the requirements for wearable sensors is that they work with low energy consumption, ideally with an integrated energy harvester like a thermo-electric generator

(TEG) to make the system completely self-sustainable [14,15]. The proper positioning of the sensor is another important factor which decides the performance of a specific sensor [16]. In addition, sensors worn near the body or even integrated into the human body have to be either very small or flexible, necessitating an appropriate fabrication technique and/or substrate choice [17]. Among the typical flexible sensor substrates on which electronics can be printed are materials such as polyethylene terephthalate (PET), polyimide (PI) or polycarbonate (PC) [18]. Many sensors use nanoparticles, nano-composites or other nanomaterials not only to enable miniaturization, but also to create the combination of physical or chemical properties required by a specific sensor [18]. These flexible sensors can be used in the form of textile-based or epidermal sensors [19]. Miniaturized magnetic sensors can also be implanted in some cases [20].

Among the various sensors which can be used for continuous health monitoring, magnetic field micro and nano sensors enable the measuring of diverse physical properties, and they are often robust and can work with low energy consumption. Typical examples of the physical effects used by such magnetic sensors are the Hall effect, giant magnetoresistance (GMR), tunnel magnetoresistance (TMR), anisotropic magnetoresistance (AMR) and giant magnetoimpedance (GMI), as well as magnetic tunnel junctions (MTJs) and fluxgate sensors [21]. These and other magnetic effects and sensors can be used to measure, e.g., biomagnetic signals like magnetocardiography (MCG), magnetoencephalography (MEG), magnetomyography (MMG) or magnetoneurography (MNG) [22]. The most important magnetic effects used in these measurements are described in the next section.

## 2. Physical Effects Used in Magnetic Micro and Nano Sensors

### 2.1. Different Magnetic Arrangements

When a material is described as “magnetic”, it is often understood to be ferro- or ferrimagnetic. However, there are several other configurations possible.

Among the non-cooperative arrangements are dia- and paramagnetism. Diamagnetism occurs in all materials, where electrons experiencing an external magnetic field are shielding this external field by a contrary internal one. In paramagnetism, an external magnetic field orients the magnetic moments parallel to it; this order is lost when the external magnetic field vanishes [23].

In ferromagnetic materials, magnetic moments are also oriented along an external magnetic field but keep this order to a large extent when the field vanishes, and an opposite field (a coercive field) is necessary to obtain an overall magnetization of zero again. Ferromagnetic materials show this behavior only at temperatures below the Curie temperature, above which they become paramagnetic. Other typical cooperative arrangements are antiferro- and ferrimagnetism. In both cases, neighboring magnetic moments are oriented antiparallel, leading to two sublattices usually oriented parallel and antiparallel to the external magnetic field. The total magnetization, as the sum of both sublattices, is zero in antiferromagnetic cases and different from zero in ferrimagnetic cases. Both effects can be found below their respective ordering temperatures, i.e., below the Néel temperature of an antiferromagnet or the Curie temperature of a ferrimagnet, respectively [23].

Combinations of these magnetic materials and other materials in magnetic or electric fields can give rise to new effects and devices, which are briefly described in the following sub-sections.

### 2.2. Hall Effect

The Hall effect is usually described in semiconductors, but it can also occur in other non-magnetic materials. In ferromagnetic materials, it is usually described as a superposition of the “ordinary” and the “extraordinary” Hall effects.

When a current flows through a semiconductor and an external magnetic field is applied perpendicular to the current flow, a Hall electric field will occur perpendicular to the current and magnetic field, which is measured as a Hall voltage [24], as depicted in Figure 1 [25]. Hall effect devices are typically used to, e.g., measure the magnetic fields

in scientific experiments, but also industrially to measure linear and angular positions, velocity, electric currents, etc. [24].

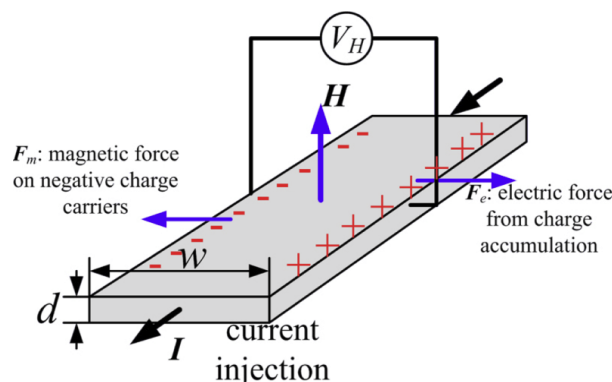


**Figure 1.** Schematic representation of a Hall device. The current  $I$  applied along the bar and the magnetic field  $H$  perpendicular to the surface result in a Hall voltage due to the force on the negative charge carriers, i.e., the electrons. Reprinted from [25], originally published under a CC-BY license.

### 2.3. Giant Magnetoresistance

Magnetoresistance effects generally describe the finding that, in some materials or material systems, electrical resistance is influenced by an applied magnetic field. After the first discoveries of relatively small effects (anisotropic magnetoresistance), which could not easily be used for precise measurements, giant magnetoresistance (GMR) was found in systems with two ferromagnetic (FM) layers separated by a nonmagnetic layer [26] and could reach values up to several hundred percent [27,28]. A simple explanation is offered by Mott’s two-fluid model (or resistor network model), depicted in Figure 2 [29]. Here, a spin-dependent scattering of the electrons in the ferromagnetic layers is assumed, where the majority spins experience less scattering than the minority spins. In typical magnetic bilayer structures (Figure 2), this leads to different overall resistances for the spin-up and spin-down electron currents in the magnetic layers and, thus, not only to a lower resistance for bilayers with a parallel magnetization orientation, but also to a higher flow of the majority electrons in this case [26].

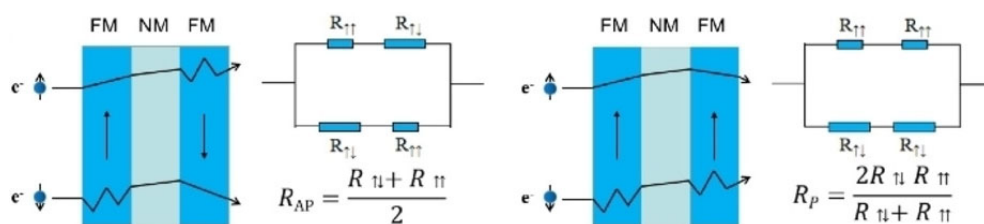


**Figure 2.** Schematic representation of the GMR effect in a resistor network model. Reprinted from [29], copyright (2023), with permission from Wiley.

### 2.4. Tunnel Magnetoresistance

Similar to GMR, tunnel magnetoresistance (TMR) consists of two ferromagnetic layers, separated by a thin insulating layer through which electrons can tunnel. Instead of spin-dependent scattering, spin-dependent band matching results in a lower electrical resistance for FM layers with parallel orientations, as shown in Figure 3 [30].

TMR sensors can also reach high resistance differences between parallel and antiparallel magnetization states of several ten to several hundred percent [31,32]. These values depend strongly on the barrier’s quality, such that technological improvements have resulted in increased TMR values [33,34].

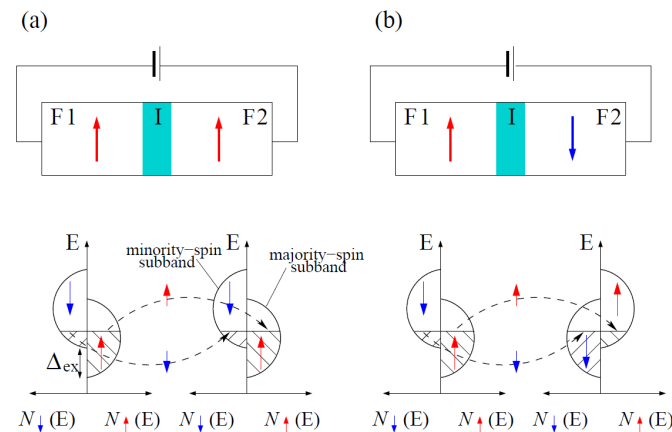


**Figure 3.** Schematic illustration of electron tunneling in ferromagnet/insulator/ferromagnet (F/I/F) tunnel junctions: (a) Parallel and (b) antiparallel orientation of magnetizations with the corresponding spin-resolved density of the d states in ferromagnetic metals that have exchange spin splitting  $\Delta_{\text{ex}}$ . Arrows in the two ferromagnetic regions are determined by the majority-spin subband. The dashed lines show spin-conserving tunneling. Reprinted with permission from [30], copyright (2004) by the American Physical Society.

### 2.5. Anisotropic and Colossal Magnetoresistance

Anisotropic magnetoresistance (AMR), as mentioned before, was firstly found to show only small changes in electric resistance depending on an external magnetic field. At present, however, very large values of AMR have been found in specific materials, such as ZrSiS, at low temperatures and with large external magnetic fields [35]. AMR can not only be found in thin films and bulk crystals, but also in nanostructures, and not only in ferromagnetic materials, but also in antiferromagnets and different manganite structures [36,37]. In the latter, the temperature dependence of AMR is different from ferromagnets, suggesting the necessity of using a model other than the Mott model in these so-called colossal magnetoresistance (CMR)-doped manganites, one which includes local uniformity [38].

### 2.6. Giant Magnetoimpedance

While magnetoresistance effects are defined by DC resistance measurements, giant magnetoimpedance (GMI) describes the large variation between the real and the imaginary part of the impedance due to an external magnetic field and is usually found in soft magnetic metals [39]. Depending on the investigated frequency range, GMI can be attributed to the magneto-inductive effect (low-frequency regime), the variation of the skin depth upon changes to its magnetic permeability (intermediate-frequency regime), or the gyromagnetic effect and ferromagnetic relaxation (high-frequency regime), respectively [40].

### 2.7. Other Magnetic Effects and Sensors

Besides these aforementioned magnetic effects which are often correlated with typical spintronics devices, there are several other possibilities for measuring physical properties using magnetic sensors [22]. In the easiest way, induction coils measure AC magnetic fields [41]. A much more sensitive magnetometer is the superconducting quantum interference device (SQUID), which consists of a superconducting loop with two Josephson junctions and measures a magnetic field perpendicular to the plane of the loop [42]. Other sensors are based on combinations of electric and magnetic fields, such as the magneto-electric magnetometer [43]; optomechanical effects, such as the cavity optomechanical magnetometer, which can be described as a combination of a Fabry–Pérot optical resonator and a mechanical resonator fixed to a magnetostrictive material [44]; and the magneto-elastic properties of magnetic wires with large magnetostriction constants [45].

Before discussing the different possibilities for constantly measuring health-related body parameters, the next section gives an overview of the different possibilities for the position of magnetic micro and nano sensors in wearables, as well as inside the body for shorter or longer durations.

### 3. Positioning Magnetic Micro and Nano Sensors for Continuous Health Monitoring

Micro and nano sensors for continuous health monitoring can be used in wearables, such as a watch or a garment, but they can also be glued on the skin like band-aid, implanted, or used as nano capsules which are swallowed or used as drugs. This section gives a brief overview of these different options for positioning a magnetic sensor near to the human body or inside it.

#### 3.1. Magnetic Sensors in Smart Textiles

Smart textiles are often used to measure ECG, pulse, breathing or other body functions [46–48]. Besides measuring the electric signals on the skin, fiber optic sensors can be used to measure respiration or the bending of joints [49]. Of the magnetic sensors, magneto-elastic fibers especially can often easily be integrated into textile fabrics. Zhao et al. reported the integration of soft magnetic fibers, produced from a silicone polymer with embedded nanomagnets, into a woven fabric with conductive silver-coated nylon fibers to form a magneto-elastic generator (MEG) which was able to measure the arterial pulse when worn on the wrist [50]. Its working principle, as depicted in Figure 4, is based on the creation of a magnetic field variation upon the deformation of the soft magnetic fibers, which in turn results in induction in the conductive yarns at the yarn intersections. The authors mentioned the advantage of such magnetic sensors' intrinsic humidity resistance, as no direct contact between skin and magnetic material is necessary [50]. Similarly, Ding et al. used magnetic/conductive composite fibers as strain sensors with potential uses in smart textiles [51].

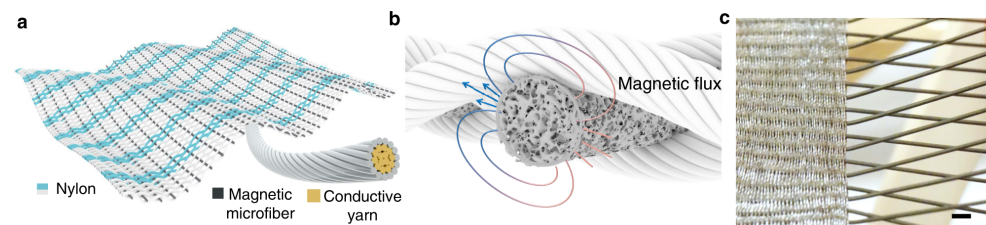


**Figure 4.** (a) Schematic design of the textile MEG; (b) schematics of the working mechanism of the textile MEG; (c) photograph of the weaving process on a loom. Reprinted from [50], originally published under a CC-BY license.

Using sewn coils from stranded wires to induce eddy currents in the torso, Teichmann et al. measured breathing and pulse by magnetic induction monitoring, as depicted in Figure 5 [52]. Magnetic induction monitoring measures the impedance distribution inside the thorax and enables the evaluation of cardiorespiratory activity from it. For this, ACs are introduced into the sensor coils, which excite AC magnetic fields, which in turn induce eddy currents in the thorax. These eddy currents induce another AC magnetic field which is measured and allows for the evaluation of changes in the thorax that are correlated with changes in the induced magnetic field, i.e., measuring breathing and pulse [52].

Instead of the integration of magnetic fibers into textile fabrics or sewing magnetic fibers onto common fabrics, magnetic sensors can also be added to garments via coating. Zhang et al., e.g., produced a proximity sensor based on magneto-straining effects by coating a spandex substrate in a magnetic layer and a subsequent conductive MXene layer [53]. Alternatively, single fibers can be coated in magnetic materials, e.g., by electroless deposition [54]. However, in most cases, coils are integrated into garments by sewing or embroidery [55–57], while more sophisticated physical principles based on magnetic effects

are scarcely found in soft, bendable textile fabrics, but in rigid wearables, as described in the next section.

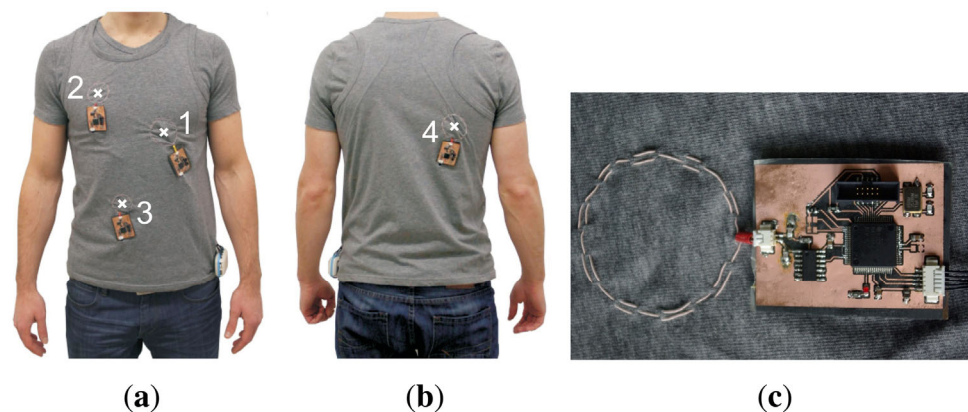


**Figure 5.** (a) Three sensors are located at the front and (b) one at the back of the thorax (coil centers are marked); (c) a close-up view of a single sensor. Reprinted from [52], originally published under a CC-BY license.

### 3.2. Magnetic Sensors in Rigid Wearables

Rigid wearables can be watches, mobile phones or similar equipment that most people use daily, but also separate devices which are preliminarily attached to clothing and could essentially be integrated after their proper miniaturization and transformation into a flexible, textile-based version.

Kunze et al. investigated the possible use of magnetic sensors in smartphones for orientation measurements of people working or doing sports [58]. Bian et al. discussed the miniaturization potential of their wearable magnetic field proximity sensor for contact tracing, compared to their prototype, to make it more comfortably wearable [59].

Huang et al. suggested monitoring people while they drive a car using a smartwatch that is tracking magnetic tags in the form of a magnetic ring and a magnetic eyeglasses clip for the head [60]. Combining a magnetic ring on the index finger with two triaxial magnetometers in a watch-like system, Friedman et al. measured wrist and hand movement [61]. A magnetic earring sensor with an embedded accelerometer was used for photoplethysmography to measure a person's heart rate during daily activities [62].

A vest with polymer boards, on which Hall effect sensors are positioned, was suggested by Wu et al. to track a medical capsule which can be used as a wireless endoscope [63]. An improved version with geomagnetic compensation which allows probands to move freely was recently suggested by Fu and Guo [64].

While these wearables are only partly integrated into daily use, in the form of watches and earrings, it is even possible to glue sensors onto the skin, as described in the next sub-section.

### 3.3. Magnetic Sensors Glued on the Skin

Magnetic sensors glued on the skin must be biocompatible, flexible, stretchable and lightweight to avoid discomfort during their use [65]. Magnetic tactile sensors enable noncontact displacement sensing through the electromagnetic induction between an AC coil and a sensing target; alternatively, Hall effect or GMR sensors can be used as tactile sensors by measuring changes in the magnetic field or magnetic flux [66]. Deformation sensing can also be performed by such a "tactile skin", e.g., one made with elastomeric silicone and embedded magnetic nanoparticles [67]. Such tactile skins can not only be used to measure joint bending, etc., or detect undesired strong magnetic fields [68], but can also improve robotic hands [69,70] and smart prosthetics [71,72]. Usually, these "skin-like" sensors are flat elastic magnetic composites, as depicted in Figure 6 [73], but there are also other shapes under investigation, such as magnetic "hair" for mechanoreception [74].

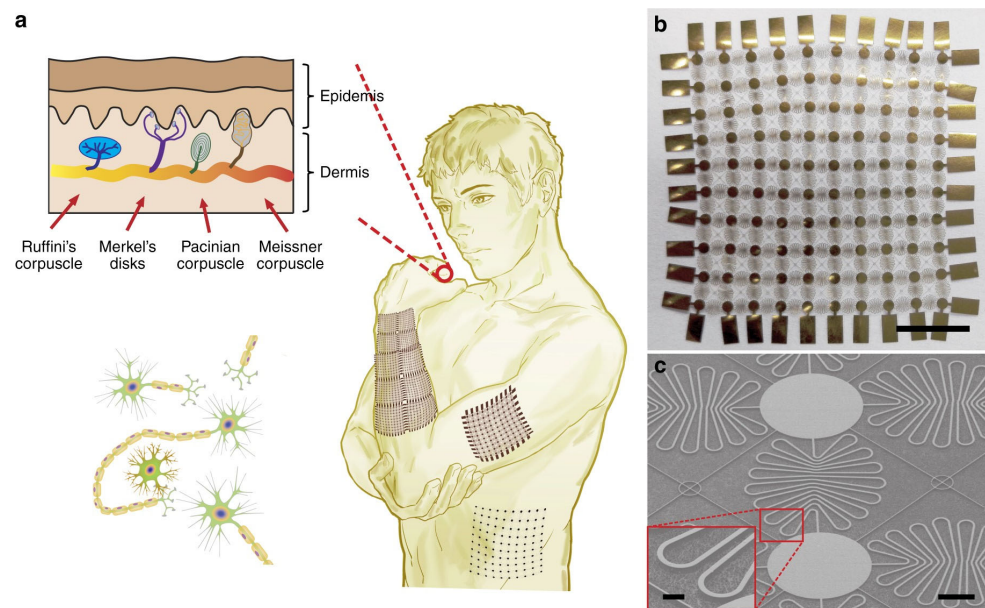


**Figure 6.** (a) Schematic of a stretchable, conformable matrix network applied to the human skin and its sensory receptors; (b) polyimide network for the application of magnetic and other sensor layers (scale bar: 5 mm); (c) scanning electron microscope (SEM) image of the matrix network (scale bar 500  $\mu\text{m}$ ). Reprinted from [73], originally published under a CC-BY license.

While the aforementioned magnetic micro and nano sensors are applied in wearables or to the skin, the next sections will describe the possibility of positioning such sensors or detectable magnetic particles inside the human body, for a limited time or for longer.

### 3.4. Magnetic Sensors in Medical Nano Capsules and for Micro-Deliveries

Magnetic particles and even sensors can be made small enough to be introduced into the bloodstream. Mathieu et al. realized the Magnetic Resonance Submarine (MR-Sub) project, in which blood vessels were examined by moving micro-devices controlled by MRI coils from the perspective of assessing cardiologic diseases. However, they called for a search for new materials, since simple metallic particles in the blood induce thrombi. Nevertheless, drug release in a given place can be supported by thermal, chemical or diffusive effects [75]. Bengal et al. used externally applied magnetic field gradients to manipulate the position of magnetic particles ranging in size from 10 nm to 10,000 nm, coming to the conclusion that larger particles move faster, while particles deposited at higher concentrations created longer chains and moved faster as well. The experiment was carried out in vivo using a the intentionally designed chip in which the magnetic field induction was equal to 0.04 T, with a gradient of 3 T/m, enabling full control of the particles' positions [76].

Magnetically responsive nano-drugs were realized by entrapping magnetic nanocrystals within a polymeric scaffold. By utilizing an external magnetic field, such capsules can be targeted and significantly enhance antitumor therapy [77–79].

### 3.5. Magnetic Capsule Endoscopy

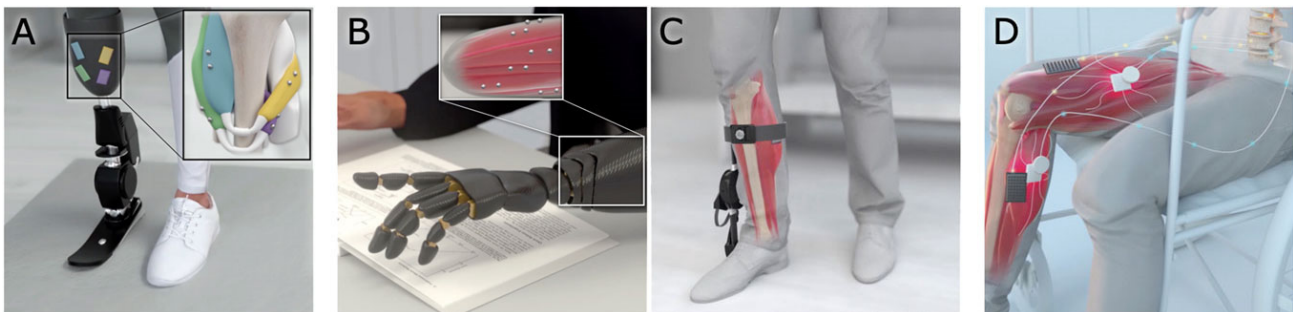
Capsule endoscopy was intensively developed further and became, in recent years, the standard tool for the noninvasive imaging of the gastrointestinal tract. Due to the development of miniaturized cameras with micro-sized light sources, as well as wireless communication systems, simple diagnosis, active therapeutics and even surgical tasks became available. Micro-robots can possess internal locomotion—based on legs—or can be externally driven by a hand-held magnet or an externally applied rotating magnetic field. These controlled pills have their own magnet on a board, usually made from neodymium–iron–boron materials. The typical parameters of endoscopic capsules are as follows: an

image registration speed of 1–30 frames/s using a CMOS sensor and VGA or HD resolutions, a camera focal length from 30 mm up to 100 mm, a power consumption of about 1–20 mW, a standard supply voltage of 3 V, a carrier frequency > 100 MHz and a data transfer rate of approx. 10 Mb/s [80–84]. It is worth mentioning that recently developed artificial intelligence (AI) methods play a key role in real-life data analysis and interpretation [85–87].

### 3.6. Implanted Magnetic Sensors

Implanting magnetic or other sensors can be the optimum solution for long-term continuous health monitoring or other long-term medical necessities. As a potential application, Tomek et al. mentioned the control of implanted gastric electrical stimulation devices by small implanted coils [88,89]. Sensor-integrated implants are a logical continuation of pure implants and can be used to detect the smallest undesired changes of the implant or its environment to enable early intervention [90]. O'Connor and Kiourti described wireless sensors implanted together with orthopedic devices, such as implants for joint replacement, which allowed for measuring the health status of the medical device and the surrounding tissue [91]. Using magnetoresistive sensors, Han et al. described the position detection of implants [92].

It is also possible to implant a pure sensor without other functional implants. An electromyography sensor system, which gathers signals from 32 implanted myoelectric sensors, was described by Weir et al., who used wireless telemetry to avoid the problems caused by percutaneous wires [93]. Taylor et al. used magnetomicrometry to track muscle tissue lengths using magnetic bead implants, e.g., for the control of a prosthetic limb device or for the muscle stimulation of paralyzed muscles, as depicted in Figure 7 [94]. Magnetic implants in the lips and tongue can be used for the silent speech recognition of patients who have lost their ability to vocalize due to injury or disease [95]. These and other implantable or wearable magnetic micro and nano sensors will be discussed in detail in the next few sections.



**Figure 7.** Applications of magnetomicrometry. When used to track muscle tissue lengths via magnetomicrometry, magnetic bead implants could enable real-time control in human–machine interfaces. (A,B) Magnetic beads implanted into residual muscles could be used to control a prosthetic limb device. (C) When implanted in a weakened muscle, magnetic beads could provide control over an exoskeleton for the restoration or augmentation of joint torque. (D) Magnetic beads in paralyzed muscles could enable closed-loop artificial muscle stimulation for the control of muscle length or force. Reprinted from [94], originally published under a CC-BY license.

## 4. Hall Effect Health Monitoring

While Hall sensors are often used in the structural health monitoring of buildings or machines [96–98], only a few examples of Hall effect sensors for medical purposes can be found in the scientific literature. Hall effect biosensors were described by Liu et al., who showed that a Hall sensor made from a single graphene layer with guanine-rich DNA immobilized on the graphene's surface had a very high potassium ion specificity and very low detection limit [99]; however, while potassium is an important substance for the human body, this sensor was not developed further for long-term measurements. Cui et al. proposed a similar graphene-based Hall effect biosensor for highly specific and

sensitive DNA detection [100]. Similarly, Noordin et al. suggested Hall effect sensors for the prediction of water pump failures in hemodialysis units [101].

A wearable Hall effect sensor was suggested by Cheng and Wilson for abnormal gait detection [102]. The authors mounted a Hall sensor with a battery and electronics near one knee and a magnet near the other one (Figure 8) to measure step length, leg gap, gait speed and a few other parameters and show that differences between normal and disturbed walking were visible in their probands.



**Figure 8.** Prototype of a wearable Hall sensor for gait monitoring. Reprinted from [102], originally published under a CC-BY license.

Jones et al. applied a Hall effect sensor in a splint used to inhibit the movement of an arthritic hand [103]. The Hall sensor was used for tactile sensing in the splinting device to support diagnosis and monitor the progression of the disease. The authors placed several sensing elements containing three-axis Hall chips and a magnet, separated by a silicone elastomer, on a hand splint and could measure the hand's closing and opening unambiguously [103].

A watch-like pulsometer based on the Hall effect was described by Lee et al. [104]. The sensor, worn on the wrist, could measure blood pressure and pulse by signal processing, with an error of around max. 20% for 13 patients with normal or high blood pressure. Another pulsometer that worked using a Hall effect device was described by Son et al., who measured pulse rate and blood pressure [105].

Especially for people working with magnetic resonance imaging (MRI) scanners, with their strong electromagnetic fields, Delmas et al. suggested a magnetic field exposure monitor that works with three orthogonal Hall sensors to monitor the static magnetic field exposure of MRI workers during a whole day [106].

While these examples show the general usability of Hall sensors for long-term health measurements, other magnetic sensors are more often used for this purpose, as described in the next few sections.

## 5. Giant Magnetoresistance Health Monitoring

While the GMR effect is often used in biomedicine, most sensors based on this effect are used in biotechnological assays, i.e., to measure biomolecule concentrations via the detection of magnetic particles [107,108]. Antarnusa et al., e.g., used  $\text{Fe}_3\text{O}_4$  nanoparticles as magnetic labels attached to streptavidin and  $\alpha$ -amylase by polyethylene glycol (PEG) to detect these labeled biomolecules using a GMR sensor [109]. To detect the influenza A virus, Krishna et al. used a GMR biosensor functionalized with 3-aminopropyltriethoxy silane (APTES) and glutaraldehyde to enable the capturing of streptavidin-labeled magnetic nanoparticles attached to target antigens, which was found to be even more sensitive than the standard enzyme-linked immunosorbent assay (ELISA) [110]. Mostufa et al.

described the use of multiplexed assays to detect cancer biomarkers using GMR-based biosensors [111], while Nesvet et al. concentrated on the GMR analysis of circulating tumor DNA epidermal growth factor receptor mutations [112]. Other GMR-based assays have aimed at GMR-based measurements of the albumin level in human blood and urine [113] of C-reactive protein, a blood biomarker [114], or generally aimed at creating other multiplex assays for proteins, etc., [115] and other microfluidic devices for the detection of magnetically labeled biomaterials [116].

There have also been, however, several attempts to use GMR sensors for long-term health monitoring. Ha et al. described the possibility of integrating a printed GMR sensor into a 3  $\mu\text{m}$  thin, highly stretchable polymer foil [117]. They used a magnetic paste with multilayered  $[\text{Py}/\text{Cu}]_{30}$  microflakes in a poly(styrene-butadiene-styrene) (SBS) elastomer, where the latter serves as a good binder to the polymeric foil. Within this structure, magnetic fields as low as 0.88 mT could be detected. This ultrafine sensor could be directly applied to the skin, as depicted in Figure 9, but it was also proposed for textiles and other wearables [117].

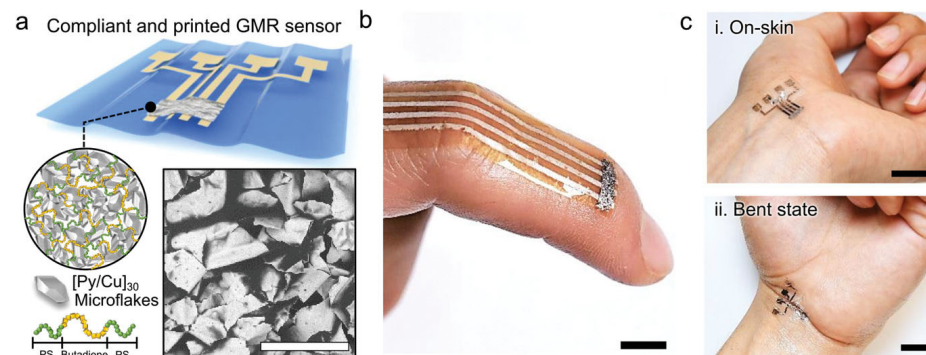


**Figure 9.** (a) Schematic illustration of GMR sensors consisting of  $[\text{Py}/\text{Cu}]_{30}$  microflakes and a copolymer (SBS) printed on ultrathin foils. SEM image reveals dried GMR paste printed on a Mylar foil. Scale bar: 100  $\mu\text{m}$ . (b) Photograph of printed GMR sensors conformably applied to skin with the curved body part of a finger. (c) Photographs of the sensor glued on a stretched (c-i) and bent (c-ii) wrist. Scale bars: 1 cm. Reprinted from [117], originally published under a CC-BY license.

GMR sensors are often applied for magnetocardiography (MCG), i.e., for magnetic measurements of electric heart activity. An example of such measurements on different torso positions was shown by Pannetier-Lecoeur et al., who compared the electric and magnetic measurements of ECG and MCG, respectively, as depicted in Figure 10 [118]. While the ECG signal looks clearer and less noisy, it must be mentioned that the MCG signal was taken with a distance of 25–30 mm between the sensor and skin [118], i.e., avoiding the necessity of skin contact with a very low contact resistance, as is necessary for common ECG measurements in wearables [46,48]. Several other researchers have reported similar MCG measurements, usually with the GMR sensor placed outside the clothes of the proband, in this way showing the main advantage of a magnetic measurement as opposed to a common ECG measurement [119–121]. Besides the MCG or, simply, the pulse rate, other GMR-based sensors have been developed to measure respiration rates [120–122] or blood pressure [121,123].

In addition to these cardiovascular parameters, other medical applications of GMR sensors can be found in the literature. Gooneratne et al., e.g., analyzed the distribution of a magnetic fluid used in magnetic fluid hyperthermia (MFH) therapy using a GMR sensor [124]. The knowledge of this distribution enabled the optimization of the MFH therapy since the homogeneous heating of a tumor necessitates knowledge of the injected magnetic fluid's distribution. For this application, the GMR probe had to be inserted into the human body via a minimally-invasive operation [124].

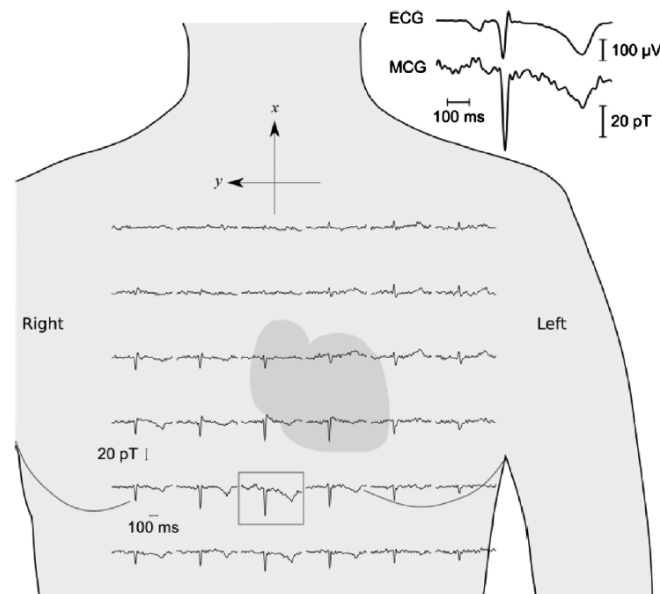


**Figure 10.** MCG signals measured at multiple locations on a single subject. The enclosed MCG trace is shown, enlarged, alongside the ECG signal. Passband 0.1–40 Hz. The position of the traces with respect to the heart is only approximate. Reprinted from [118], copyright (2011), with permission from AIP.

Caruso investigated, in his doctoral thesis, the possibility of the local magnetic detection of neuronal currents and showed some magnetic recordings of neuronal activity in a cat's cerebral cortex using a GMR sensor; however, some questions remained open, such as the difference between the expected and measured signal height as well as the difference between the AC and DC signal height [125].

## 6. Tunnel Magnetoresistance Health Monitoring

Tunnel magnetoresistance sensors are especially used to measure low magnetic fields, and they can often be found in biomedical applications [126]. Magnetic nanoparticles are used as biomarkers, generating stray fields which influence the magnetic moments in one layer of the TMR element, while the target molecules binding on the nanoparticle surface modify these stray fields and can thus be measured, as depicted in Figure 11 [127]. Lei et al., e.g., demonstrated measurements of low concentrations of magnetic nanoparticles attached to human chorionic gonadotropin using a TMR sensor [128]. In the case of *E. coli* detection by a TMR biosensor, the bacteria were labeled with magnetic beads, resulting in its high sensitivity and their rapid detection [129]. Similarly, carboxyl-modified  $\text{Fe}_3\text{O}_4$  nanoparticles with anti-ricin monoclonal antibodies were used for the TMR-based detection of ricin [130], and other biomarkers with magnetic beads as labels have successfully been detected by TMR sensors [131–133]. It should be mentioned that the detection of magnetite nanoparticles in the air, i.e., of atmospheric pollution, is also possible using TMR sensors [134].

For the detection of the magnetic FeCrNbB nanoparticles in cancer cells, in magnetic hyperthermia therapy, Ghemes et al. suggested a TMR sensor which was tested in a lab environment outside the human body as a proof of concept [135]. A TMR sensor in an eyeglass frame was used to detect eye blinking, e.g., was usable for eyelid gesture control, via a thin magnetic strip on the eyelid [136]. Alternatively, Tanwear et al. combined a TMR sensor in an eyeglass frame with a small magnet in a contact lens to detect eye movements, which could be used for human–machine interactions [137].

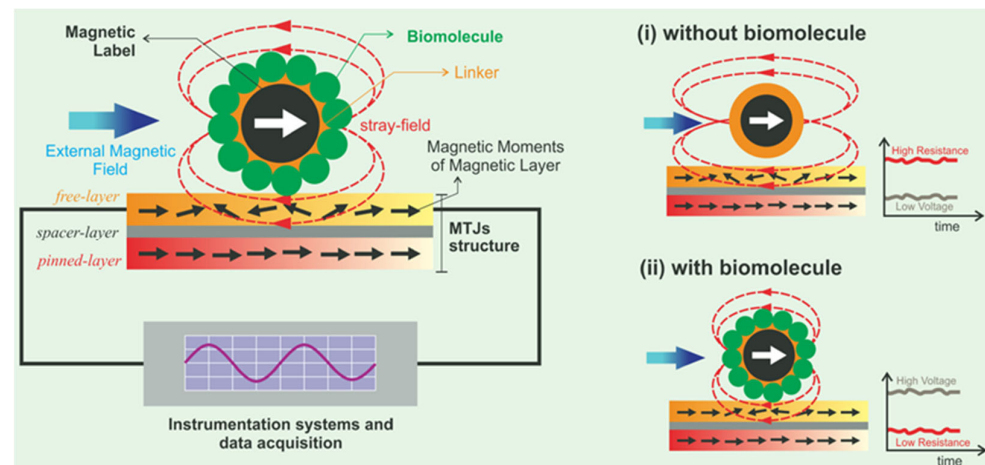


**Figure 11.** Schematic illustration of biomolecule detection mechanism. Reprinted from [127], originally published under a CC-BY license.

TMR sensors were also suggested for the detection of implants. Khokle et al. described the high-resolution detection of the micromotion of an orthopedic implant by an eddy current loop coupled with a TMR sensor, enabling the *in vivo* detection of these micromotions to reduce revision surgeries after the mechanical failure of an implant [138].

Preclinic studies in a swine model showed that a TMR sensor could detect dextran-coated iron oxide nanoparticles injected into the lymph nodes, so that a sentinel lymph node which needs to be removed after metastasis formation could easily be located [139].

Besides GMR and TMR, there are also some health monitoring applications based on AMR, as described in the next section.

## 7. Anisotropic Magnetoresistance Health Monitoring

While the AMR effect is smaller than the GMR and TMR effects, AMR sensors can nevertheless resolve magnetic fields below the mT range and are easier to produce since their layer thicknesses are less critical, and permalloy (Py), as a simple material, can be used for their production [140]. Since AMR sensors can also be printed, they can be prepared on ultrathin polymer foils, which makes them bendable and usable for on-skin applications [141,142]. Oliveros Mata et al. showed that an AMR sensor printed using a magnetic paste of Py/Ta flakes and an SBS copolymer on a thin polymer film could detect sub-mT magnetic fields and did not even change its magnetoresistive properties after bending and folding, as depicted in Figure 12 [143]. Wang et al. even found a detection limit of 150 nT for their flexible AMR sensor [144]. The flexibility of an AMR sensor on a Kapton substrate was investigated by Chen et al., who found good anti-fatigue behavior after bending 500 times and suggested using such sensors in wearables for potential health-related applications [145]. Similarly, Su et al. reported no impact of bending state on the AMR effect of epitaxial CoFe films on flexible mica substrates [146]. Combining an AMR sensor with a radio frequency identification (RFID) chip, Sorli et al. could measure variations of the earth's magnetic field and detect movements of the human body from these measurements, by their comparison with recorded motion data, in this way enabling the monitoring of a person's activity during rehabilitation [147].

It should be mentioned that biomedical applications based on the detection of magnetic biomarkers normally do not use AMR sensors, most probably since bending and folding are not necessary in these applications. On the other hand, only a few reports of *in vivo* measurements with AMR sensors can be found in the literature. Vera et al., e.g., used a biocompatible PDMS-coated AMR sensor as an implantable neural interface to detect the small magnetic signals from neural activity, tested as subcutaneous sensor in a rat model [148]. Weitschies et al. measured the disintegration of tablets with iron oxide magnetic markers, in a simulated *in vivo* environment, by an AMR sensor [149], while

other groups used AMR sensors to monitor the solid dosage form of a magnetically labeled dosage in the gastrointestinal tract [150,151]. AMR sensors were also used by Placidi et al., who mentioned that GMR sensors would have approx.  $5\times$  higher sensitivity ( $\sim 10\ \mu\text{G}$ , as opposed to  $\sim 50\ \mu\text{G}$  for AMR devices) but often an integrated flux concentrator in the form of a thin FM layer, which would make directional measurements complicated, which is why they chose AMR devices to follow an endovascular catheterization in vivo [152]. Similarly, Paixao et al. combined AMR with AC biosusceptometry to measure gastrointestinal motility and found a high correlation, in in vivo studies, between this system and manometry techniques [153]. Arami et al. suggested integrating AMR sensors into the polyethylene insert of a total knee prosthesis combined with a permanent magnet attached to the femoral part of the prosthesis, in this way enabling the collection of kinematic information about the prosthetic knee [154].

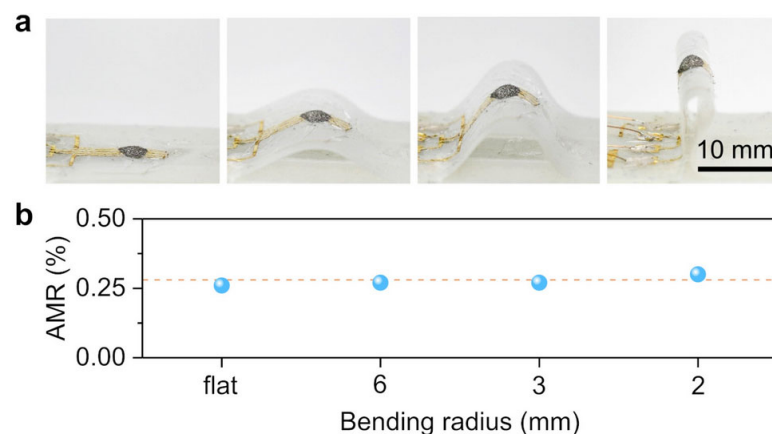


**Figure 12.** (a) Bending states of the sensor and (b) its respective AMR responses, measured at  $\pm 400$  mT. Reprinted from [143], originally published under a CC-BY license.

Besides the aforementioned special applications, only a few reports of in vivo AMR sensor applications can be found in the scientific literature. In particular, MCG and respiratory measurements, which are often performed by GMR sensors, are usually not conducted with AMR sensors.

## 8. Colossal Magnetoresistance Health Monitoring

Only a few reports on colossal magnetoresistance sensors in the field of health monitoring can be found in the literature. De et al. reported on typical CMR materials, i.e., lanthanum calcium manganite ( $\text{La}_{0.7}\text{Sr}_{0.3}\text{MnO}_3$ ) with and without  $\text{Eu}^{3+}$  doping, used to show antimicrobial properties without using them in a CMR sensor [155]. These  $\text{La}_{0.7}\text{Sr}_{0.3}\text{MnO}_3$  thin films were also used for body temperature measurements, again without using a CMR sensor [156]. The idea of using  $\text{La}_{0.7}\text{Sr}_{0.3}\text{MnO}_3$  as a thermometer was also discussed by Wu et al., who also measured the CMR effect of their samples, but did not mention its potential application in health monitoring [157]. Carrier et al. mentioned that several perovskites showing CMR are lead-free which enables, in principle, their use in vivo, but without giving examples of their health monitoring applications [158]. Besides these and very similar studies, no mentions of health monitoring in correlation with CMR were found.

## 9. Giant Magnetoimpedance Health Monitoring

Magnetoimpedance sensors can be used for different health monitoring applications, such as the localization of the biomagnetic fields generated by muscles, the heart beat or brain activity [159]. Karnaushenko et al., e.g., suggested a new method to realize arrays of GMI sensors to enable magneto-encephalography measurements using GMR-based magnetic field gradiometers [160]. To enable respiration monitoring, Thiabgoh et al. suggested a microwire coil magneto-LC resonance sensor with coils from  $\text{Co}_{69.25}\text{Fe}_{4.25}\text{Si}_{13}\text{B}_{12.5}\text{Nb}_1$  microwires, which

show a GMI effect [161]. It should be mentioned that this system was applied not in wearables, but above the bed of a patient who has a small permanent magnet attached to his breast (cf. Figure 13), whose smallest position changes—e.g., by breathing—could be measured by the GMI sensor at a distance of 3–15 cm [161]. Similarly, Wu et al. developed tactile sensors based on GMI sensors [71].

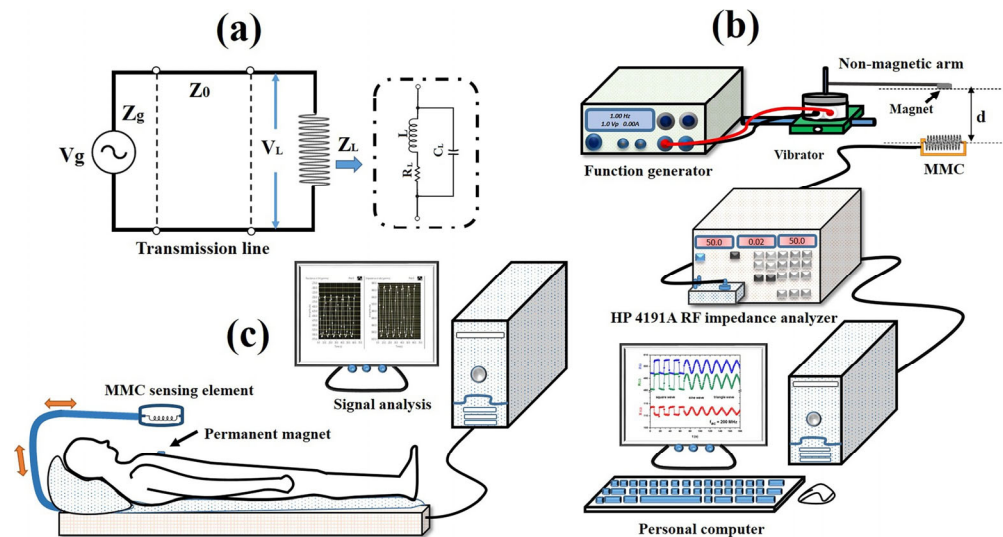


**Figure 13.** (a) An equivalent circuit; (b) experimental setup for a magnetic coil sensor; (c) principle operation of magnetic microwire coil based on the GMI effect for a noncontact respiration rate monitoring device. Reprinted with permission from [161], copyright (2017) by Elsevier.

Kobayashi et al. tested a 64-channel GMI sensor system for MCG measurements in comparison with a SQUID magnetometer and found similar signals, while the GMI system did not necessitate working at liquid helium temperatures in a magnetically shielded room, as the SQUID does [162].

Furthermore, with a very thin and flexible GMI sensor, which could measure magnetic fields from 22 nT to 400 mT, Li et al. could detect the geomagnetic field as well as positional relationships between the sensor and a fixed permanent magnet, which they suggested for the rehabilitation training of the fingers' motoric function [68].

Besides these point-of-care- and rehabilitation-related applications of the GMI effect, there are also several biosensors reported in the literature. Both the detection of magnetic markers and label-free detection due to GMI changes from surface modifications are possible, enabling the detection of small amounts of biomolecules [163,164]. As an example, Zhu et al. described the detection of cancer biomarkers by an ultra-sensitive GMI sensor [165]. Wang et al. showed that a low number of only 10 magnetic beads in a microcavity could be detected by a GMI sensor in contact with this microcavity [166]. Many other research groups have reported the detection of magnetic nanoparticles, microbeads or ferrofluids used to magnetically label biomolecules, such as cancer cells [167], C-reactive protein [168] or human papilloma virus [169].

## 10. Other Magnetic Effects and Sensors for Health Monitoring

Besides these aforementioned magnetic effects, a few others have occasionally been studied regarding their potential use in health monitoring.

The idea of measuring AC magnetic fields using induction coils was applied by Mahdavi and Rosell-Ferrer to measure the vital signs of a sleeping patient [170]. The system was placed under the mattress to avoid disturbing the patient and could measure their breathing and cardiac activity, using two foils for excitation and detection. As a special method, magnetic induction tomography (MIT) should be mentioned, which enables biomedical imaging at lower costs than X-ray tomography and magnetic resonance imaging

and without hazardous radiation [171,172]; however, this technique is not suitable for long-term health monitoring.

Magneto-electric sensors can be used for magneto-cardiography, magneto-encephalography, etc. [173–175]. For magneto-myography (MMG), Zuo et al. simulated and developed, as an alternative to a SQUID, a magneto-electric sensor which enabled the measuring of pT MMG signals [176]. Apu et al. described the potential use of magneto-electric nanoparticles in drug delivery, bio-imaging, neural stimulation and other biomedical applications [177]. Combining energy harvesting and sensing with a magneto-electric antenna, Das et al. modeled such a hybrid antenna as a potential neural implant [178].

The SQUID, while able to measure very low fields, operates at the temperature of liquid helium and is thus not suitable for wearable applications [162]; however, it can be used as a gold standard for comparison with other biomagnetic measurement methods [179]. It is also valid for cavity optomechanical magnetometers [180].

### 11. Conclusions and Outlook

Different magnetic sensors can be used for continuous health monitoring. Several of them can be miniaturized to create wearability, either in textile fabrics, watches or glued on the skin, or to enable implantation or transporting them through the human body. The typical magnetic effects which are often used are the Hall effect, GMR, TMR, AMR and GMI, in addition to less often utilized magnetic properties. Due to their specific properties, sensors based on these effects have different advantages and corresponding areas of application, as exemplarily given here: biotechnological assays (Hall effect, GMR, TMR, GMI), gait monitoring and the movement of fingers and other body parts (Hall effect, TMR, AMR, GMI), blood pressure and pulse measurements (Hall effect), magnetocardiography and respiration (GMR, GMI), magnetic nanobead localization in hyperthermia therapy (GMR, TMR), the localization of a catheter in vivo (AMR), the micromotion detection of implants (TMR, AMR), measurements of neural activity (AMR), etc. A brief overview of the sensors discussed in this review, with their respective operation ranges, is given in Table 1.

**Table 1.** Overview of magnetic micro and nano sensors for health monitoring.

Physical Effect	Application
Hall effect	Biosensor—detection of DNA, etc.
Hall effect	Gait detection, hand movement, pulsimeter, magnetic field exposure
GMR	Biotechnological assays—biomolecule concentration with magnetic labels
GMR	Magnetocardiography, respiration rate, blood pressure
GMR	Magnetic fluid detection in hyperthermia therapy
TMR	Biotechnology—biomarker detection with magnetic beads as labels
TMR	Detection of magnetic nanoparticles in hyperthermia therapy
TMR	Detection of implants
AMR	Movement detection during rehabilitation
AMR	Detection of neural activity (implanted)
AMR	Kinematic information about prosthesis
GMI	Measuring biomagnetic fields of muscles, heart or brain, breathing sensors
GMI	Finger motion detection during rehabilitation
GMI	Biosensors for label-free detection of cancer biomarkers
GMI	Detection of magnetically labeled biomolecules

While many applications of these sensors in continuous health monitoring have already been developed, there is still research needed regarding the combination of higher-sensitivity sensor devices and, at the same time, smaller and more flexible sensors to enable optimum comfort while patients use them on long time scales. In the future, especially the continuous health monitoring of the elderly will become more and more important to enable them living autonomously for as long as possible without the risk of an undetected serious heart problem or other potentially fatal health problems. Besides using magnetic sensors to immediately detect an emergency, magnetic micro and nano sensors can also be

expected to be used more and more in cancer treatment and other point-of-care applications to improve medical treatments.

**Author Contributions:** Conceptualization, T.B. and G.E.; methodology, T.B., A.E. and G.E.; validation, T.B., I.K. and G.E.; investigation, T.B., K.G. and A.E.; writing—original draft preparation, T.B. and A.E.; writing—review and editing, all authors; visualization, G.E.; supervision, G.E. All authors have read and agreed to the published version of the manuscript.

**Funding:** This research received no external funding.

**Institutional Review Board Statement:** Not applicable.

**Informed Consent Statement:** Not applicable.

**Data Availability Statement:** No data were created in this review paper.

**Conflicts of Interest:** Author Karoline Guenther was employed by the company Saurer Spinning Solutions GmbH & Co. The remaining authors declare no conflicts of interest.

## References

- Teixeira, E.; Fonseca, H.; Diniz-Sousa, F.; Veras, L.; Boppre, G.; Oliveira, J.; Pinto, D.; Alves, A.J.; Barbosa, A.; Mendes, R.; et al. Wearable Devices for Physical Activity and Healthcare Monitoring in Elderly People: A Critical Review. *Geriatrics* **2021**, *6*, 38. [[CrossRef](#)] [[PubMed](#)]
- Fernández-Ballesteros, R.; Robine, J.M.; Walker, A.; Kalache, A. Active Aging: A Global Goal. *Curr. Gerontol. Geriatr. Res.* **2013**, *2013*, 298012. [[CrossRef](#)] [[PubMed](#)]
- Koch, S. Healthy ageing supported by technology—A cross-disciplinary research challenge. *Inform. Health Soc. Care* **2010**, *35*, 81–91. [[CrossRef](#)] [[PubMed](#)]
- Souza do Nascimento, L.M.; Bonfati, L.V.; La Banca Freitas, M.; Alves Mendes, J.J., Jr.; Siqueira, H.V.; Stevan, S.L., Jr. Sensors and Systems for Physical Rehabilitation and Health Monitoring—A Review. *Sensors* **2020**, *20*, 4063. [[CrossRef](#)] [[PubMed](#)]
- Li, H.; Shrestha, A.; Heidari, H.; Kernec, J.L.; Fioranelli, F. A Multisensory Approach for Remote Health Monitoring of Older People. *IEEE J. Electromagn. RF Microw. Med. Biol.* **2018**, *2*, 102–108. [[CrossRef](#)]
- Chen, Y.; Shen, C. Performance Analysis of Smartphone-Sensor Behavior for Human Activity Recognition. *IEEE Access* **2017**, *5*, 3095–3110. [[CrossRef](#)]
- Chen, S.W.; Qi, J.M.; Fan, S.C.; Qiao, Z.; Yeo, J.C.; Lim, C.T. Flexible Wearable Sensors for Cardiovascular Health Monitoring. *Adv. Healthc. Mater.* **2021**, *10*, 2100116. [[CrossRef](#)] [[PubMed](#)]
- Han, F.; Wang, T.S.; Liu, G.Z.; Liu, H.; Xie, X.Y.; Wie, Z.; Li, J.; Jiang, C.; He, Y.; Xu, F. Materials with Tunable Optical Properties for Wearable Epidermal Sensing in Health Monitoring. *Adv. Mater.* **2022**, *34*, 2109055. [[CrossRef](#)]
- Anikwe, C.V.; Nweke, H.F.; Ikegwu, A.C.; Egwuonwu, C.A.; Onu, F.U.; Alo, U.R.; The, Y.W. Mobile and wearable sensors for data-driven health monitoring system: State-of-the-art and future prospect. *Expert Syst. Appl.* **2022**, *202*, 117362. [[CrossRef](#)]
- Henderson, J.; Condell, J.; Connolly, J.; Kelly, D.; Curran, K. Review of Wearable Sensor-Based Health Monitoring Glove Devices for Rheumatoid Arthritis. *Sensors* **2021**, *21*, 1576. [[CrossRef](#)]
- Li, W.-D.; Ke, K.; Jia, J.; Pu, J.-H.; Zhao, X.; Bao, R.-Y.; Liu, Z.-Y.; Bai, L.; Zhang, K.; Yang, M.-B.; et al. Recent Advances in Multiresponsive Flexible Sensors towards E-skin: A Delicate Design for Versatile Sensing. *Small* **2022**, *18*, 2103734. [[CrossRef](#)] [[PubMed](#)]
- Sujith, A.V.L.N.; Sajja, G.S.; Mahalakshmi, V.; Nuhmani, S.; Prasanalakshmi, B. Systematic review of smart health monitoring using deep learning and Artificial intelligence. *Neurosci. Inform.* **2022**, *2*, 1000028. [[CrossRef](#)]
- AlShorman, O.; AlShorman, B.; Al-khassaweneh, M.; Alkahtani, F. A review of internet of medical things (IoMT)-based remote health monitoring through wearable sensors: A case study for diabetic patients. *Indones. J. Electr. Eng. Comput. Sci.* **2020**, *20*, 414–422. [[CrossRef](#)]
- Kim, J.Y.; Khan, S.; Wu, P.; Park, S.J.; Park, H.J.; Yu, C.H.; Kim, W.C. Self-charging wearables for continuous health monitoring. *Nano Energy* **2021**, *79*, 105419. [[CrossRef](#)]
- Zhang, X.; Ai, J.W.; Zou, R.P.; Su, B. Compressible and Stretchable Magnetoelectric Sensors Based on Liquid Metals for Highly Sensitive, Self-Powered Respiratory Monitoring. *ACS Appl. Mater. Interfaces* **2021**, *13*, 15727–15737. [[CrossRef](#)]
- Nasiri, S.; Khosravani, M.R. Progress and challenges in fabrication of wearable sensors for health monitoring. *Sens. Actuators A Phys.* **2020**, *312*, 112105. [[CrossRef](#)]
- Sreenilayam, S.P.; Ul Ahad, I.; Nicolosi, V.; Garzon, V.A.; Brabazon, D. Advanced materials of printed wearables for physiological parameter monitoring. *Mater. Today* **2020**, *32*, 147–177. [[CrossRef](#)]
- Peng, B.; Zhao, F.N.; Ping, J.F.; Ying, Y.B. Recent Advances in Nanomaterial-Enabled Wearable Sensors: Material Synthesis, Sensor Design, and Personal Health Monitoring. *Small* **2020**, *16*, 2002681. [[CrossRef](#)] [[PubMed](#)]
- Khoshmanesh, F.; Thurgood, P.; Pirogova, E.; Nahavandi, S.; Baratchi, S. Wearable sensors: At the frontier of personalised health monitoring, smart prosthetics and assistive technologies. *Biosens. Bioelectron.* **2021**, *176*, 112946. [[CrossRef](#)]

20. Zuo, S.M.; Heidari, H.; Farina, D.; Nazarpour, K. Miniaturized Magnetic Sensors for Implantable Magnetomyography. *Adv. Mater. Technol.* **2020**, *5*, 2000185. [[CrossRef](#)]
21. Mostufa, S.; Yari, P.; Rezaei, B.; Xu, K.L.; Wu, K. Flexible Magnetic Field Nanosensors for Wearable Electronics: A Review. *ACS Appl. Nano Mater.* **2023**, *6*, 13732–13765. [[CrossRef](#)]
22. Murzin, D.; Mapps, D.J.; Levada, K.; Belyaev, V.; Omelyanchik, A.; Panina, L.; Rodionova, V. Ultrasensitive Magnetic Field Sensors for Biomedical Applications. *Sensors* **2020**, *20*, 1569. [[CrossRef](#)]
23. Reis, M. *Fundamentals of Magnetism*; Elsevier: Oxford, UK, 2013.
24. Popovic, R.S. *Hall Effect Devices*; Institute of Physics Publishing: Bristol, UK; CRC Press: Boca Raton, FL, USA, 2003.
25. Khan, M.A.; Sun, J.; Li, B.D.; Przybysz, A.; Kosel, J. Magnetic sensors-A review and recent technologies. *Eng. Res. Express* **2021**, *3*, 022005. [[CrossRef](#)]
26. Thompson, S.M. The discovery, development and future of GMR: The Nobel Prize 2007. *J. Phys. D Appl. Phys.* **2008**, *41*, 093001. [[CrossRef](#)]
27. Garcia, N.; Munoz, M.; Zhao, Y.W. Magnetoresistance in excess of 200% in Ballistic Ni Nanocontacts at Room Temperature and 100 Oe. *Phys. Rev. Lett.* **1999**, *82*, 2923. [[CrossRef](#)]
28. Parkin, S.S.P.; Li, Z.G.; Smith, D.J. Giant magnetoresistance in antiferromagnetic Co/Cu multilayers. *Appl. Phys. Lett.* **1991**, *58*, 2710–2712. [[CrossRef](#)]
29. Zhu, Y.N.; Jiang, Q.L.; Zhang, J.; Ma, Y.G. Recent Progress of Organic Semiconductor Materials in Spintronics. *Chem.–Asian J.* **2023**, *18*, e202201125. [[CrossRef](#)] [[PubMed](#)]
30. Zutic, I.; Fabian, J.; Das Sarma, S. Spintronics: Fundamentals and applications. *Rev. Mod. Phys.* **2004**, *76*, 323. [[CrossRef](#)]
31. Yuasa, S.; Fukushima, A.; Nagahama, T.; Ando, K.; Suzuki, Y. High Tunnel Magnetoresistance at Room Temperature in Fully Epitaxial Fe/MgO/Fe Tunnel Junctions due to Coherent Spin-Polarized Tunneling. *Jpn. J. Appl. Phys.* **2004**, *43*, L588. [[CrossRef](#)]
32. Parkin, S.S.P.; Kaiser, C.; Panchula, A.; Rice, P.M.; Hughes, B.; Samant, M.; Yang, S.-H. Giant tunnelling magnetoresistance at room temperature with MgO (100) tunnel barriers. *Nat. Mater.* **2004**, *3*, 862–867. [[CrossRef](#)]
33. Bowen, M.; Cros, V.; Petroff, F.; Fert, A.; Martínez Boubeta, C.; Costa-Krämer, J.L.; Anguita, J.V.; Cebollada, A.; Briones, F.; de Teresa, J.M.; et al. Large magnetoresistance in Fe/MgO/FeCo(001) epitaxial tunnel junctions on GaAs(001). *Appl. Phys. Lett.* **2001**, *79*, 1655–1657. [[CrossRef](#)]
34. Djayaprawira, D.D.; Tsunekawa, K.; Nagai, M.; Maehara, H.; Yamagata, S.; Watanabe, N.; Yuasa, S.; Suzuki, Y.; Ando, K. 230% room-temperature magnetoresistance in CoFeB/MgO/CoFeB magnetic tunnel junctions. *Appl. Phys. Lett.* **2005**, *86*, 09202. [[CrossRef](#)]
35. Lv, Y.-Y.; Zhang, B.-B.; Li, X.; Yao, S.-H.; Chen, Y.B.; Zhou, J.; Zhang, S.-T.; Lu, M.-H.; Chen, Y.-F. Extremely large and significantly anisotropic magnetoresistance in ZrSiS single crystals. *Appl. Phys. Lett.* **2016**, *108*, 244101. [[CrossRef](#)]
36. Zhao, C.-J.; Ding, L.; HuangFu, J.-S.; Zhang, J.-Y.; Yu, G.-H. Research progress in anisotropic magnetoresistance. *Rare Met.* **2013**, *32*, 213–224. [[CrossRef](#)]
37. Fina, I.; Marti, X.; Yi, D.; Liu, J.; Chu, J.H.; Rayan-Serrao, C.; Suresha, S.; Shick, A.B.; Zelezny, J.; Junghwirth, T.; et al. Anisotropic magnetoresistance in an antiferromagnetic semiconductor. *Nat. Commun.* **2014**, *5*, 4671. [[CrossRef](#)] [[PubMed](#)]
38. Yau, J.-B.; Hong, X.; Posadas, A.; Ahn, C.H.; Gao, W.; Altman, E.; Bason, Y.; Klein, L.; Sidorov, M.; Krivokapic, Z. Anisotropic magnetoresistance in colossal magnetoresistive La<sub>1-x</sub>Sr<sub>x</sub>NiO<sub>3</sub> thin films. *J. Appl. Phys.* **2007**, *102*, 103901. [[CrossRef](#)]
39. Knobel, M.; Vázquez, M.; Kraus, L. Giant Magnetoimpedance. *Handb. Magn. Mater.* **2003**, *15*, 497–563.
40. Phan, M.-H.; Peng, H.-X. Giant magnetoimpedance materials: Fundamentals and applications. *Prog. Mater. Sci.* **2008**, *53*, 323–420. [[CrossRef](#)]
41. Mooney, J.W.; Ghasemi-Roudsari, S.; Banham, E.R.; Symonds, C.; Pawlowski, N.; Varcoe, B.T.H. A portable diagnostic device for cardiac magnetic field mapping. *Biomed. Phys. Eng. Express* **2017**, *3*, 015008. [[CrossRef](#)]
42. Clarke, J.; Weinstock, H. *SQUID Sensors: Fundamentals, Fabrication and Applications*, 1st ed.; Weinstock, H., Ed.; Springer: Berlin/Heidelberg, Germany, 1996.
43. Wang, Y.J.; Gao, J.Q.; Li, M.H.; Shen, Y.; Hasanyan, D.; Li, J.F.; Viehland, D. A review on equivalent magnetic noise of magnetolectric laminate sensors. *Philos. Trans. R. Soc. A Math. Phys. Eng. Sci.* **2014**, *372*, 20120455. [[CrossRef](#)]
44. Li, B.-B.; Bulla, D.; Prakash, V.; Forstne, S.; Dehghan-Manshadi, A.; Dunlop, H.R.; Foster, S.; Bowen, W.P. Scalable high-sensitivity optomechanical magnetometers on a chip. *APL Photonics* **2018**, *3*, 120806. [[CrossRef](#)]
45. Ren, L.; Yu, K.; Tan, Y. Wireless and Passive Magnetoelastic-Based Sensor for Force Monitoring of Artificial Bone. *IEEE Sens. J.* **2019**, *19*, 2096–2104. [[CrossRef](#)]
46. Blachowicz, T.; Ehrmann, G.; Ehrmann, A. Textile-Based Sensors for Biosignal Detection and Monitoring. *Sensors* **2021**, *21*, 6042. [[CrossRef](#)] [[PubMed](#)]
47. Singha, K.; Kumar, J.; Pandit, P. Recent Advancements in Wearable & Smart Textiles: An Overview. *Mater. Today Proc.* **2019**, *16*, 1518–1523.
48. Trummer, S.; Ehrmann, A.; Büsgen, A. Development of underwear with integrated 12 channel ECG for men and women. *AUTEX Res. J.* **2017**, *17*, 344–349. [[CrossRef](#)]
49. Massaroni, C.; Saccomandi, P.; Schena, E. Medical Smart Textiles Based on Fiber Optic Technology: An Overview. *J. Funct. Biomater.* **2015**, *6*, 204–221. [[CrossRef](#)] [[PubMed](#)]

50. Zhao, X.; Zhou, Y.H.; Xu, J.; Chen, G.R.; Fang, Y.S.; Tat, T.; Xiao, X.; Song, Y.; Li, S.; Chen, J. Soft fibers with magnetoelasticity for wearable electronics. *Nat. Commun.* **2021**, *12*, 6755. [[CrossRef](#)]
51. Ding, L.; Xuan, S.H.; Feng, J.B.; Gong, X.L. Magnetic/conductive composite fibre: A multifunctional strain sensor with magnetically driven property. *Compos. Part A Appl. Sci. Manuf.* **2017**, *100*, 97–105. [[CrossRef](#)]
52. Teichmann, D.; Kuhn, A.; Leonhardt, S.; Walter, M. The MAIN Shirt: A Textile-Integrated Magnetic Induction Sensor Array. *Sensors* **2014**, *14*, 1039–1056. [[CrossRef](#)]
53. Zhang, W.G.; Guo, Q.H.; Duan, Y.; Xing, C.Y.; Peng, Z.C. A Textile Proximity/Pressure Dual-Mode Sensor Based on Magneto-Straining and Piezoresistive Effects. *IEEE Sens. J.* **2022**, *22*, 10420–10427. [[CrossRef](#)]
54. Chen, L.M.; Lu, M.Y.; Wang, Y.Q.; Huang, Y.H.; Zhu, S.; Tang, J.W.; Zhu, C.; Liu, X.Q.; Yin, W.L. Whole System Design of a Wearable Magnetic Induction Sensor for Physical Rehabilitation. *Adv. Intell. Syst.* **2019**, *1*, 1900037. [[CrossRef](#)]
55. Mecnika, V.; Hoerr, M.; Krievins, I.; Jockenhoevel, S.; Gries, T. Technical Embroidery for Smart Textiles: Review. *Mater. Sci. Text. Cloth. Technol.* **2014**, *9*, 56–63. [[CrossRef](#)]
56. Gi, S.O.; Lee, Y.J.; Koo, H.R.; Khang, S.N.; Kim, K.-N.; Kang, S.-J.; Lee, J.H.; Lee, J.-W. Application of a Textile-based Inductive Sensor for the Vital Sign Monitoring. *J. Electr. Eng. Technol.* **2014**, *9*, 742–749. [[CrossRef](#)]
57. Grabham, N.J.; Li, Y.; Clare, L.R.; Stark, B.H.; Beeby, S.P. Fabrication Techniques for Manufacturing Flexible Coils on Textiles for Inductive Power Transfer. *IEEE Sens. J.* **2018**, *18*, 2599–2606. [[CrossRef](#)]
58. Kunze, K.; Bahle, G.; Lukowicz, P.; Partidge, K. Can magnetic field sensors replace gyroscopes in wearable sensing applications? In Proceedings of the International Symposium on Wearable Computers (ISWC) 2010, Seoul, Republic of Korea, 10–13 October 2010; pp. 1–4.
59. Bian, S.Z.; Zhou, B.; Lukowicz, P. Social Distance Monitor with a Wearable Magnetic Field Proximity Sensor. *Sensors* **2020**, *20*, 5101. [[CrossRef](#)] [[PubMed](#)]
60. Huang, H.; Chen, H.K.; Lin, S. MagTrack: Enabling Safe Driving Monitoring with Wearable Magnetics. In Proceedings of the MobiSys '19: Proceedings of the 17th Annual International Conference on Mobile Systems, Applications, and Services, Seoul, Republic of Korea, 17–21 June 2019; pp. 326–339.
61. Friedman, N.; Rowe, J.B.; Reinkensmeyer, D.J.; Bachmann, J. The Manometer: A Wearable Device for Monitoring Daily Use of the Wrist and Fingers. *IEEE J. Biomed. Health Inform.* **2014**, *18*, 1804–1812. [[CrossRef](#)]
62. Poh, M.-Z.; Swenson, N.C.; Picard, R.W. Motion-tolerant magnetic earring sensor and wireless earpiece for wearable photoplethysmography. *IEEE Trans. Inf. Technol. Biomed.* **2010**, *14*, 786–794. [[CrossRef](#)] [[PubMed](#)]
63. Wu, X.D.; Hou, W.S.; Peng, C.L.; Zheng, X.L.; Fang, X.; He, J. Wearable magnetic locating and tracking system for MEMS medical capsule. *Sens. Actuators A Phys.* **2008**, *141*, 432–439. [[CrossRef](#)]
64. Fu, Y.M.; Guo, Y.-X. Wearable Permanent Magnet Tracking System for Wireless Capsule Endoscope. *IEEE Sens. J.* **2022**, *22*, 8113–8122. [[CrossRef](#)]
65. Almansouri, A.S.; Alsharif, N.A.; Khan, M.A.; Swanepoel, L.; Kaidarova, A.; Salama, K.N.; Kosel, J. An Imperceptible Magnetic Skin. *Adv. Mater. Technol.* **2019**, *4*, 1900493. [[CrossRef](#)]
66. Wang, C.G.; Liu, C.; Shang, F.F.; Niu, S.Y.; Ke, L.N.; Zhang, N.; Ma, B.B.; Li, R.Z.; Sun, X.; Zhang, S. Tactile sensing technology in bionic skin: A review. *Biosens. Bioelectron.* **2023**, *220*, 114882. [[CrossRef](#)]
67. Hellebrekers, T.; Kroemer, O.; Majidi, C. Soft Magnetic Skin for Continuous Deformation Sensing. *Adv. Intell. Syst.* **2019**, *1*, 1900025. [[CrossRef](#)]
68. Li, S.B.; Wu, Y.Z.; Asghar, W.; Li, F.L.; Zhang, Y.; He, Z.D.; Liu, J.Y.; Wang, Y.W.; Liao, M.Y.; Shang, J.; et al. Wearable Magnetic Field Sensor with Low Detection Limit and Wide Operation Range for Electronic Skin Applications. *Adv. Sci.* **2023**, *10*, 2304525.
69. Yan, Y.C.; Hu, Z.; Yang, Z.B.; Yuan, W.H.; Song, C.Y.; Pan, J.; Shen, Y.J. Soft magnetic skin for super-resolution tactile sensing with force self-decoupling. *Sci. Robot.* **2021**, *6*, eabc8801. [[CrossRef](#)] [[PubMed](#)]
70. Roberts, P.; Zadan, M.; Majidi, C. Soft Tactile Sensing Skins for Robotics. *Curr. Robot. Rep.* **2021**, *2*, 343–354. [[CrossRef](#)]
71. Wu, Y.; Liu, Y.; Zhou, Y.; Man, Q.; Hu, C.; Asghar, W.; Li, F.; Yu, Z.; Shang, J.; Liu, G.; et al. A skin-inspired tactile sensor for smart prosthetics. *Sci. Robot.* **2018**, *3*, eaat0429. [[CrossRef](#)] [[PubMed](#)]
72. Weathersby, E.J.; Gurrey, C.J.; McLean, J.B.; Sanders, B.N.; Larsen, B.G.; Carter, R.; Garbini, J.L.; Sanders, J.E. Thin Magnetically Permeable Targets for Inductive Sensing: Application to Limb Prosthetics. *Sensors* **2019**, *19*, 4041. [[CrossRef](#)]
73. Hua, Q.L.; Sun, J.L.; Liu, H.T.; Bao, R.R.; Yu, R.M.; Zhai, J.Y.; Pan, C.F.; Wang, Z.L. Skin-inspired highly stretchable and conformable matrix networks for multifunctional sensing. *Nat. Commun.* **2018**, *9*, 244. [[CrossRef](#)] [[PubMed](#)]
74. Becker, C.; Bao, B.; Karnaushenko, D.D.; Bandari, V.K.; Rivkin, B.; Li, Z.; Faghieh, M.; Karnaushenko, D.; Schmidt, O.G. A new dimension for magnetosensitive e-skins: Active matrix integrated micro-origami sensor arrays. *Nat. Commun.* **2022**, *13*, 2121. [[CrossRef](#)] [[PubMed](#)]
75. Mathieu, J.B.; Soulez, G.; Martel, S. Potential Applications of Untethered Microdevices in the Blood Vessels within the Constraints of an MRI System. In Proceedings of the 2005 IEEE Engineering in Medicine and Biology 27th Annual Conference, Shanghai, China, 17–18 January 2005; pp. 4850–4853.
76. Benhal, P.; Broda, A.; Najafali, D.; Malik, P.; Mohammed, A.; Ramaswamy, B.; Depireux, D.A.; Shimoji, M.; Shukoor, M.; Shapiro, B. On-chip testing of the speed of magnetic nano- and micro-particles under a calibrated magnetic gradient. *J. Magn. Magn. Mat.* **2019**, *474*, 187–198. [[CrossRef](#)]

77. Xie, A.; Hanif, S.; Ouyang, J.; Tang, Z.; Kong, N.; Kim, N.Y.; Qi, B.; Patel, D.; Shi, B.; Tao, W. Stimuli-responsive prodrug-based cancer nanomedicine. *eBioMedicine* **2020**, *56*, 102821. [[CrossRef](#)]
78. Kainz, Q.M.; Reiser, O. Polymer- and Dendrimer-Coated Magnetic Nanoparticles as Versatile Supports for Catalysts, Scavengers, and Reagents. *Acc. Chem. Res.* **2014**, *47*, 667–677. [[CrossRef](#)] [[PubMed](#)]
79. Yang, H.-W.; Hua, M.-Y.; Liu, H.-L.; Huang, C.-Y.; Tsai, R.-Y.; Lu, Y.-J.; Chen, H.-J.; Tang, H.-J.; Hsien, H.-Y.; Chang, Y.-S.; et al. Self-protecting core-shell magnetic nanoparticles for targeted, traceable, long half-life delivery of BCNU to gliomas. *Biomaterials* **2011**, *32*, 6523–6532. [[CrossRef](#)] [[PubMed](#)]
80. Han Kim, S.; Chun Jai, H. Capsule Endoscopy: Pitfalls and Approaches to Overcome. *Diagnostics* **2021**, *11*, 1765. [[CrossRef](#)] [[PubMed](#)]
81. O’Hara, F.; McNamara, D. Small-Bowel Capsule Endoscopy—Optimizing Capsule Endoscopy in Clinical Practice. *Diagnostics* **2021**, *11*, 2139. [[CrossRef](#)]
82. Solitano, V.; Zilli, A.; Franchellucci, G.; Alloca, M.; Fiorino, G.; Furfaro, F.; D’Amico, F.; Danase, S.; Al Awadhi, S. Artificial Endoscopy and Inflammatory Bowel Disease: Welcome to the Future. *J. Clinic. Med.* **2022**, *11*, 569. [[CrossRef](#)] [[PubMed](#)]
83. Estevinho, M.M.; Pinho, R.; Rodrigues, A.; Ponte, A.; Correia, J.; Mesquita, P.; Freitas, T. Capsule Enteroscopy Using the Mirocam@versus OMOM@Systems: A Matched Case–Control Study. *Life* **2023**, *13*, 1809. [[CrossRef](#)] [[PubMed](#)]
84. Levartovsky, A.; Eliakim, R. Video Capsule Endoscopy Plays an Important Role in the Management of Crohn’s Disease. *Diagnostics* **2023**, *13*, 1507. [[CrossRef](#)] [[PubMed](#)]
85. Tziortziotis, I.; Laskaratos, F.-M.; Coda, S. Role of Artificial Intelligence in Video Capsule Endoscopy. *Diagnostics* **2021**, *11*, 1192. [[CrossRef](#)]
86. Moen, S.; Vuik, S.E.R.; Kuipers, E.J.; Spaander, M.C.W. Artificial Intelligence in Colon Capsule Endoscopy—A Systematic Review. *Diagnostics* **2022**, *12*, 1994. [[CrossRef](#)]
87. Mascarenhas, M.; Martins, M.; Afonso, J.; Ribeiro, T.; Cardoso, P.; Mendes, F.; Andrade, P.; Cardoso, H.; Ferreira, J.; Macedo, G. The Future of Minimally Invasive Capsule Panendoscopy: Robotic Precision, Wireless Imaging and AI-Driven Insights. *Cancers* **2023**, *15*, 5861. [[CrossRef](#)]
88. Tomek, J.; Mlejnek, P.; Janásek, V.; Ripka, P.; Kaspar, P.; Chen, J. Gastric Motility and Volume Sensing by Implanted Magnetic Sensors. *Sens. Lett.* **2007**, *5*, 276–278. [[CrossRef](#)]
89. Tomek, J.; Mlejnek, P.; Janásek, V.; Ripka, P.; Kaspar, P.; Chen, J. The precision of gastric motility and volume sensing by implanted magnetic sensors. *Sens. Actuators A Phys.* **2008**, *142*, 34–39. [[CrossRef](#)]
90. Veletic, M.; Apu, E.H.; Simic, M.; Bergsland, J.; Balasingham, I.; Contag, C.H.; Ashammakhi, N. Implants with Sensing Capabilities. *Chem. Rev.* **2022**, *122*, 16329–16363. [[CrossRef](#)] [[PubMed](#)]
91. O’Connor, C.; Kiourti, A. Wireless Sensors for Smart Orthopedic Implants. *J. Bio-Tribo-Corros.* **2017**, *3*, 20. [[CrossRef](#)]
92. Han, W.; Chau, K.T.; Jiang, C.Q.; Liu, W. Accurate Position Detection in Wireless Power Transfer Using Magnetoresistive Sensors for Implant Applications. *EEE Trans. Magn.* **2018**, *54*, 4001205.
93. Weir, R.F.; Troyk, P.R.; DeMichele, G.A.; Kerns, D.A.; Schorsch, J.F.; Maas, H. Implantable Myoelectric Sensors (IMESs) for Intramuscular Electromyogram Recording. *IEEE Trans. Biomed. Eng.* **2009**, *56*, 159–171. [[CrossRef](#)] [[PubMed](#)]
94. Taylor, C.R.; Clark, W.H.; Clarrissimeaux, E.G.; Yeon, S.H.; Carty, M.J.; Lipsitz, S.R.; Bronson, R.T.; Roberts, T.J.; Herr, H.M. Clinical viability of magnetic bead implants in muscle. *Front. Bioeng. Biotechnol.* **2022**, *10*, 1010276. [[CrossRef](#)] [[PubMed](#)]
95. Hofe, R.; Ell, S.R.; Fagan, M.J.; Gilbert, J.M.; Green, P.D.; Moore, R.K.; Rybchenko, S.I. Small-vocabulary speech recognition using a silent speech interface based on magnetic sensing. *Speech Commun.* **2013**, *55*, 22–32. [[CrossRef](#)]
96. Angelopoulos, S.; Misiaris, D.; Banis, G.; Liang, K.; Tsarabaris, P.; Ktena, A.; Hristoforou, E. Steel health monitoring device based on Hall sensors. *J. Magn. Magn. Mater.* **2020**, *515*, 167304. [[CrossRef](#)]
97. Addabbo, T.; Fort, A.; Mugnaini, M.; Panzardi, E.; Pozzebon, A.; Tani, M.; Vignoli, V. A low cost distributed measurement system based on Hall effect sensors for structural crack monitoring in monumental architecture. *Measurement* **2018**, *116*, 652–657. [[CrossRef](#)]
98. Verma, A.K.; Akkulu, P.; Padmanabhan, S.V.; Radhika, S. Automatic Condition Monitoring of Industrial Machines Using FSA-Based Hall-Effect Transducer. *IEEE Sens. J.* **2021**, *21*, 1072–1081. [[CrossRef](#)]
99. Liu, X.Q.; Ye, C.; Li, X.Q.; Cui, N.Y.; Wu, T.Z.; Du, S.Y.; Wie, Q.P.; Fu, L.; Yin, J.C.; Lin, C.-T. Highly Sensitive and Selective Potassium Ion Detection Based on Graphene Hall Effect Biosensors. *Materials* **2018**, *11*, 399. [[CrossRef](#)] [[PubMed](#)]
100. Cui, N.Y.; Wang, F.; Ding, H.Y. Graphene-Based Hall Effect Biosensor for Improved Specificity and Sensitivity of Label-Free DNA Detection. *Nano* **2020**, *15*, 2050088. [[CrossRef](#)]
101. Noordin, M.K.; Amran, M.E.; Bani, N.A.; Ahmad Kamil, A.S.; Md Nasir, A.N.; Arsat, M. Failure Prediction for Hemodialysis Units Using Machine Learning and Hall Effect Sensors. In Proceedings of the 2023 IEEE 2nd National Biomedical Engineering Conference (NBEC), Melaka, Malaysia, 5–7 September 2023; pp. 170–175.
102. Chheng, C.; Wilson, D. Abnormal Gait Detection Using Wearable Hall-Effect Sensors. *Sensors* **2021**, *21*, 1206. [[CrossRef](#)] [[PubMed](#)]
103. Jones, D.; Wang, L.F.; Ghanbari, A.; Vardakastani, V.; Kedgley, A.E.; Gardiner, M.D.; Vincent, T.L.; Culmer, P.R.; Alazmani, A. Design and Evaluation of Magnetic Hall Effect Tactile Sensors for Use in Sensorized Splints. *Sensors* **2020**, *20*, 1123. [[CrossRef](#)] [[PubMed](#)]
104. Lee, S.-S.; Choi, J.-G.; Son, I.-H.; Kim, K.-H.; Nam, D.-H.; Hong, Y.-S.; Lee, W.-B.; Hwang, D.-G.; Rhee, J.-R. Fabrication and Characterization of a Wrist Wearable Cuffless Pulsimeter by Using the Hall Effect Device. *J. Magn.* **2011**, *16*, 449–452. [[CrossRef](#)]

105. Son, I.-H.; Kim, K.-H.; Choi, J.-G.; Nam, D.-H.; Lee, S.-S. Measurement and Analysis of Pulse Wave Using a Clamping Pulsimeter Equipped With Hall Effect Device. *IEEE Trans. Magn.* **2011**, *47*, 3063–3065. [[CrossRef](#)]
106. Delmas, A.; Belguerras, L.; Weber, N.; Odille, F.; Pasquier, C.; Felblinger, J.; Vuissoz, P.-A. Calibration and non-orthogonality correction of three-axis Hall sensors for the monitoring of MRI workers' exposure to static magnetic fields. *Bio Electro Magn.* **2018**, *39*, 108–119. [[CrossRef](#)]
107. Wu, K.; Tonini, D.; Liang, S.; Saha, R.; Chugh, V.K.; Wang, J.-P. Giant Magnetoresistance Biosensors in Biomedical Applications. *ACS Appl. Mater. Interfaces* **2022**, *14*, 9945–9969. [[CrossRef](#)]
108. Weiss, R.; Mattheis, R.; Reiss, G. Advanced giant magnetoresistance technology for measurement applications. *Meas. Sci. Technol.* **2013**, *24*, 082001. [[CrossRef](#)]
109. Antarnusa, G.; Elda Swastika, P.; Suharyadi, E. Wheatstone bridge-giant magnetoresistance (GMR) sensors based on Co/Cu multilayers for bio-detection applications. *J. Phys. Conf. Ser.* **2018**, *1011*, 012061. [[CrossRef](#)]
110. Krishna, V.D.; Wu, K.; Perez, A.M.; Wang, J.-P. Giant Magnetoresistance-based Biosensor for Detection of Influenza A Virus. *Front. Microbiol.* **2016**, *7*, 400. [[CrossRef](#)]
111. Mostufa, S.; Rezaei, B.; Yari, P.; Xu, K.L.; Gómez-Pastora, J.; Sun, J.J.; Shi, Z.Q.; Wu, K. Giant Magnetoresistance Based Biosensors for Cancer Screening and Detection. *ACS Appl. Bio Mater.* **2023**, *6*, 4042–4059. [[CrossRef](#)]
112. Nesvet, J.C.; Antilla, K.A.; Pancirer, D.S.; Lozano, A.X.; Preiss, J.S.; Ma, W.J.; Fu, A.H.; Park, S.-M.; Gambhir, S.S.; Fan, A.C.; et al. Giant Magnetoresistive Nanosensor Analysis of Circulating Tumor DNA Epidermal Growth Factor Receptor Mutations for Diagnosis and Therapy Response Monitoring. *Clin. Chem.* **2021**, *67*, 534–542. [[CrossRef](#)] [[PubMed](#)]
113. Wibowo, N.A.; Riyanto, C.A.; Suharyadi, E.; Sabarman, H. Giant Magnetoresistance Sensor for Rapid and Simple Bovine Serum Albumin Assay With Ag-Functionalized Iron Oxide Nanoparticles Label. *IEEE Sens. J.* **2023**, *23*, 9204–9209. [[CrossRef](#)]
114. Meng, F.; Zhang, L.; Huo, W.S.; Lian, J.; Jesorka, A.; Shi, X.Z.; Gao, Y.H. Dynamic Range Expansion of the C-Reactive Protein Quantification with a Tandem Giant Magnetoresistance Biosensor. *ACS Omega* **2021**, *6*, 12923–12930. [[CrossRef](#)] [[PubMed](#)]
115. Wang, Y.; Wang, W.; Yu, L.; Tu, L.; Feng, Y.L.; Klein, T.; Wang, J.-P. Giant magnetoresistive-based biosensing probe station system for multiplex protein assays. *Biosens. Bioelectron.* **2015**, *70*, 61–68. [[CrossRef](#)]
116. Ger, T.-R.; Wu, P.-S.; Wang, W.-J.; Chen, C.-A.; Abu, P.A.R.; Chen, S.-L. Development of a Microfluidic Chip System with Giant Magnetoresistance Sensor for High-Sensitivity Detection of Magnetic Nanoparticles in Biomedical Applications. *Biosensors* **2023**, *13*, 807. [[CrossRef](#)]
117. Ha, M.J.; Canón Bermúdez, G.S.; Kosub, T.; Mönch, I.; Zabala, Y.; Oliveros Mata, E.S.; Illing, R.; Wang, Y.K.; Fassbender, J.; Makarov, D. Printable and Stretchable Giant Magnetoresistive Sensors for Highly Compliant and Skin-Conformal Electronics. *Adv. Mater.* **2021**, *33*, 2005521. [[CrossRef](#)]
118. Pannetier-Lecoœur, M.; Parkkonen, L.; Sergeeva-Chollet, N.; Polovy, H.; Fermon, C.; Fowley, C. Magnetocardiography with sensors based on giant magnetoresistance. *Appl. Phys. Lett.* **2011**, *98*, 153705. [[CrossRef](#)]
119. Kalyan, K.; Chugh, V.K.; Anoop, C.S. Non-invasive heart rate monitoring system using giant magneto resistance sensor. In Proceedings of the 2016 38th Annual International Conference of the IEEE Engineering in Medicine and Biology Society (EMBC), Orlando, FL, USA, 16–20 August 2016; pp. 4873–4876.
120. Jishnu, K.; Anoop, C.S. A Simple Bio-Instrumentation Platform for Vital-Sign Estimation Using MagnetoPlethysmography. In Proceedings of the 2023 International Conference on Power, Instrumentation, Energy and Control (PIECON), Aligarh, India, 10–12 February 2023; pp. 1–5.
121. Sarkar, S. Design of Magnetic Sensor Based All-in-One Cardiorespiratory Health Monitoring System. In Proceedings of the 2020 42nd Annual International Conference of the IEEE Engineering in Medicine & Biology Society (EMBC), Montreal, QC, Canada, 20–24 July 2020; pp. 4660–4663.
122. Chugh, V.K.; Kalyan, K.; Anoop, C.S. Feasibility study of a giant Magneto-Resistance based respiration rate monitor. In Proceedings of the 2016 38th Annual International Conference of the IEEE Engineering in Medicine and Biology Society (EMBC), Orlando, FL, USA, 16–20 August 2016; pp. 2327–2330.
123. Chugh, V.K.; Kalyan, K.; Anoop, C.S.; Patra, A.; Negi, S. Analysis of a GMR-based plethysmograph transducer and its utility for real-time Blood Pressure measurement. In Proceedings of the 2017 39th Annual International Conference of the IEEE Engineering in Medicine and Biology Society (EMBC), Jeju, Republic of Korea, 11–15 July 2017; pp. 1704–1707.
124. Gooneratne, C.P.; Kurnicki, A.; Yamada, S.; Mukhopadhyay, S.C.; Kosel, J. Analysis of the Distribution of Magnetic Fluid inside Tumors by a Giant Magnetoresistance Probe. *PLoS ONE* **2013**, *8*, e81227. [[CrossRef](#)]
125. Caruso, L. Giant magnetoresistance Based Sensors for Local Magnetic Detection of Neuronal Currents. Ph.D. Thesis, Université Pierre et Marie Curie—Paris VI, Paris, France, 2015.
126. Ren, C.H.; Bayin, Q.G.; Feng, S.L.; Fu, Y.S.; Ma, X.; Guo, J.H. Biomarkers detection with magnetoresistance-based sensors. *Biosens. Bioelectron.* **2020**, *165*, 112340. [[CrossRef](#)]
127. Wibowo, N.A.; Kurniawan, C.; Kusumahastuti, D.K.A.; Setiawan, A.; Suharyadi, E. Review—Potential of Tunneling Magnetoresistance Coupled to Iron Oxide Nanoparticles as a Novel Transducer for Biosensors-on-Chip. *J. Electrochem. Soc.* **2024**, *171*, 017512. [[CrossRef](#)]
128. Lei, H.M.; Wang, K.; Ji, X.J.; Cui, D.X. Contactless Measurement of Magnetic Nanoparticles on Lateral Flow Strips Using Tunneling Magnetoresistance (TMR) Sensors in Differential Configuration. *Sensors* **2016**, *16*, 2130. [[CrossRef](#)]

129. Wu, Y.Z.; Liu, Y.W.; Zhan, Q.F.; Liu, J.P.; Li, R.-W. Rapid detection of Escherichia coli O157:H7 using tunneling magnetoresistance biosensor. *AIP Adv.* **2017**, *7*, 056658. [[CrossRef](#)]
130. Mu, X.-H.; Liu, H.-F.; Tong, Z.-Y.; Du, B.; Liu, S.; Liu, B.; Liu, Z.-W.; Gao, C.; Wang, J.; Dong, H. A new rapid detection method for ricin based on tunneling magnetoresistance biosensor. *Sens. Actuators B Chem.* **2019**, *284*, 638–649. [[CrossRef](#)]
131. Albon, C.; Weddemann, A.; Auge, A.; Rott, K.; Hütten, A. Tunneling magnetoresistance sensors for high resolution particle detection. *Appl. Phys. Lett.* **2009**, *95*, 023101. [[CrossRef](#)]
132. Amara, S.; Bu, R.; Alawein, M.; Alsharif, N.; Khan, M.A.; Wen, Y.; Zhang, X.X.; Kosel, J.; Fariborzi, H. Highly-Sensitive Magnetic Tunnel Junction Based Flow Cytometer. In Proceedings of the 2018 IEEE International Symposium on Medical Measurements and Applications (MeMeA), Rome, Italy, 11–13 June 2018; pp. 1–5.
133. Lian, J.; Chen, S.; Qiu, Y.Q.; Zhang, S.H.; Shi, S.; Gao, Y.H. A fully automated in vitro diagnostic system based on magnetic tunnel junction arrays and superparamagnetic particles. *J. Appl. Phys.* **2012**, *111*, 07B315. [[CrossRef](#)]
134. Amara, S.; Aljedaibi, A.; Alrashoudi, A.; Mbarek, S.B.; Khan, D.; Massoud, Y. High-performance MTJ-based sensors for monitoring of atmospheric pollution. *AIP Adv.* **2023**, *13*, 035329. [[CrossRef](#)]
135. Ghemes, C.; Dragos-Pinzaru, O.-G.; Tibu, M.; Lostun, M.; Lupu, N.; Chiriac, H. Tunnel Magnetoresistance-Based Sensor for Biomedical Application: Proof-of-Concept. *Coatings* **2023**, *13*, 227. [[CrossRef](#)]
136. Tanwear, A.; Heidari, H.; Paz, E.; Böhnert, T.; Ferreira, R. Eyelid Gesture Control using Wearable Tunneling Magnetoresistance Sensors. In Proceedings of the 2020 27th IEEE International Conference on Electronics, Circuits and Systems (ICECS), Glasgow, UK, 23–25 November 2020; pp. 1–4.
137. Tanwear, A.; Liang, X.P.; Liu, Y.C.; Vuckovic, A.; Ghannam, R.; Böhnert, T.; Paz, E.; Freitas, P.P.; Ferreira, R.; Heidari, H. Spintronic Sensors Based on Magnetic Tunnel Junctions for Wireless Eye Movement Gesture Control. *IEEE Trans. Biomed. Circuits Syst.* **2020**, *14*, 1299–1310. [[CrossRef](#)]
138. Khokle, R.P.; Franco, F.; de Freitas, S.C.; Esselle, K.P.; Heimlich, M.C.; Bokor, D.J. Eddy Current–Tunneling Magneto-Resistive Sensor for Micromotion Detection of a Tibial Orthopaedic Implant. *IEEE Sens. J.* **2019**, *19*, 1285–1292. [[CrossRef](#)]
139. Cousins, A.; Balalis, G.L.; Thompson, S.K.; Forero Morales, D.; Mohtar, A.; Wedding, A.B.; Thierry, B. Novel Handheld Magnetometer Probe Based on Magnetic Tunneling Junction Sensors for Intraoperative Sentinel Lymph Node Identification. *Sci. Rep.* **2015**, *5*, 10842. [[CrossRef](#)]
140. Cañón Bermúdez, G.S.; Fuchs, H.; Bischoff, L.; Fassbender, J.; Makarov, D. Electronic-skin compasses for geomagnetic field-driven artificial magnetoreception and interactive electronics. *Nat. Electron.* **2018**, *1*, 589. [[CrossRef](#)]
141. Ge, J.; Wang, X.; Drack, M.; Volkov, O.; Liang, M.; Cañón Bermúdez, G.S.; Illing, R.; Wang, C.; Zhou, S.; Fassbender, J.; et al. A bimodal soft electronic skin for tactile and touchless interaction in real time. *Nat. Commun.* **2019**, *10*, 4405. [[CrossRef](#)]
142. Wang, C.; Su, W.; Pu, J.; Hu, Z.; Liu, M. A Self-biased Anisotropic Magnetoresistive (AMR) Magnetic Field Sensor on Flexible Kapton. In Proceedings of the 2018 IEEE International Magnetism Conference (INTERMAG), Singapore, 23–27 April 2018; p. 1.
143. Oliveros Mata, E.S.; Cañón Bermúdez, G.S.; Ha, M.J.; Kosub, T.; Zabala, Y.; Fassbender, J.; Makarov, D. Printable anisotropic magnetoresistance sensors for highly compliant electronics. *Appl. Phys. A* **2021**, *127*, 280. [[CrossRef](#)]
144. Wang, Z.G.; Wang, X.J.; Li, M.H.; Gao, Y.; Hu, Z.Q.; Nan, T.X.; Liang, X.F.; Chen, H.H.; Yang, J.; Cash, S.; et al. Highly Sensitive Flexible Magnetic Sensor Based on Anisotropic Magnetoresistance Effect. *Adv. Mater.* **2016**, *28*, 9370–9377. [[CrossRef](#)] [[PubMed](#)]
145. Chen, Y.N.; Zhao, D.Y.; Shao, J.; Fu, Z.; Wang, C.Y.; Wang, S.P.; Du, J.; Zhong, M.C.; Duan, J.B.; Li, Y.; et al. Highly flexible anisotropic magnetoresistance sensor for wearable electronics. *Rev. Sci. Instrum.* **2023**, *94*, 045005. [[CrossRef](#)]
146. Su, G.-Y.; You, M.-C.; Chuang, K.-W.; Wu, M.-H.; Hsieh, C.-H.; Lin, C.-Y.; Yang, C.-Y.; Anbalagan, A.K.; Lee, C.-H. Investigating Anisotropic Magnetoresistance in Epitaxially Strained CoFe Thin Films on a Flexible Mica. *Nanomaterials* **2023**, *13*, 3154. [[CrossRef](#)]
147. Sorli, B.; Vena, A.; Belaizi, Y.; Balde, M. UHF RFID anisotropic magnetoresistance sensor for human motion monitoring. In Proceedings of the 2015 IEEE International Instrumentation and Measurement Technology Conference (I2MTC) Proceedings, Pisa, Italy, 11–14 May 2015; pp. 1165–1168.
148. Vera, A.; Martínez, I.; Enger, L.G.; Guillet, B.; Guerrero, R.; Diez, J.M.; Rousseau, O.; Chok Sing, M.L.; Pierron, V.; Perna, P.; et al. High-Performance Implantable Sensors based on Anisotropic Magnetoresistive  $\text{La}_{0.67}\text{Sr}_{0.33}\text{MnO}_3$  for Biomedical Applications. *ACS Biomater. Sci. Eng.* **2023**, *9*, 1020–1029. [[CrossRef](#)]
149. Weitschies, W.; Hartmann, V.; Grützmann, R.; Breitzkreutz, J. Determination of the disintegration behavior of magnetically marked tablets. *Eur. J. Pharm. Biopharm.* **2001**, *52*, 221–226. [[CrossRef](#)] [[PubMed](#)]
150. Andrä, W.; Danan, H.; Kirmsse, W.; Kramer, H.H.; Saupe, P.; Schmieg, R.; Bellemann, M.E. A novel method for real-time magnetic marker monitoring in the gastrointestinal tract. *Phys. Med. Biol.* **2000**, *45*, 3081–3093. [[CrossRef](#)] [[PubMed](#)]
151. Weitschies, W.; Blume, H.; Mönnikes, H. Magnetic marker monitoring: High resolution real-time tracking of oral solid dosage forms in the gastrointestinal tract. *Eur. J. Pharm. Biopharm.* **2010**, *74*, 93–101. [[CrossRef](#)] [[PubMed](#)]
152. Placidi, G.; Franchi, D.; Gallo, P.; Sotgiu, A. Design of a Magnetic Localisation System for In-Vivo Endovascular Interventions. In Proceedings of the 2007 29th Annual International Conference of the IEEE Engineering in Medicine and Biology Society, Lyon, France, 22–26 August 2007; pp. 499–503.
153. Paixao, F.C.; Corá, L.A.; Américo, M.F.; de Oliveira, R.B.; Baffa, O.; Miranda, J.R.A. Development of an AMR-ACB Array for Gastrointestinal Motility Studies. *IEEE Trans. Biomed. Eng.* **2012**, *59*, 2737–2743. [[CrossRef](#)] [[PubMed](#)]
154. Arami, A.; Simoncini, M.; Atasoy, O.; Ali, S.; Hasenkamp, W.; Bertsch, A.; Meurville, E.; Tanner, S.; Renaud, P.; Dehollain, C.; et al. Instrumented Knee Prosthesis for Force and Kinematics Measurements. *IEEE Trans. Autom. Sci. Eng.* **2013**, *10*, 615–624. [[CrossRef](#)]

155. De, D.; Mandal, S.M.; Gauri, S.G.; Bhattacharya, R.; Ram, S.; Roy, S.K. Antibacterial Effect of Lanthanum Calcium Manganate ( $\text{La}_{0.67}\text{Ca}_{0.33}\text{MnO}_3$ ) Nanoparticles Against *Pseudomonas aeruginosa* ATCC 27853. *J. Biomed. Nanotechnol.* **2010**, *6*, 138–144. [CrossRef]
156. Hou, W.X.; Yao, Y.F.; Li, Y.J.; Peng, B.; Shi, K.Q.; Zhou, Z.Y.; Pan, J.Y.; Liu, M.; Hu, J.F. Linearly shifting ferromagnetic resonance response of  $\text{La}_{0.7}\text{Sr}_{0.3}\text{MnO}_3$  thin film for body temperature sensors. *Front. Mater. Sci.* **2022**, *16*, 220589. [CrossRef]
157. Wu, S.; Fadil, D.; Liu, S.; Aryan, A.; Renault, B.; Routoure, J.-M.; Guillet, B.; Flament, S.; Langlois, P.; Méchin, L.  $\text{La}_{0.7}\text{Sr}_{0.3}\text{MnO}_3$  Thin Films for Magnetic and Temperature Sensors at Room Temperature. *Sens. Transducers* **2012**, 253–265.
158. Carlier, T.; Ferri, A.; Saitzek, S.; Huvé, M.; Bayart, A.; Da Costa, A.; Desfeux, R.; Tebano, A. Microstructure and local electrical behavior in  $[(\text{Nd}_2\text{Ti}_2\text{O}_7)_4/(\text{SrTiO}_3)_n]_{10}$  ( $n = 4-8$ ) superlattices. *RSC Adv.* **2018**, *8*, 11262–11271. [CrossRef]
159. Jimenez, V.O.; Hwang, K.Y.; Nguyen, D.; Rahman, Y.; Albrecht, C.; Senator, B.; Thiabgoh, O.; Devkota, J.; Bui, V.D.A.; Lam, D.S.; et al. Magnetoimpedance Biosensors and Real-Time Healthcare Monitors: Progress, Opportunities, and Challenges. *Biosensors* **2022**, *12*, 517. [CrossRef]
160. Karnaushenko, D.; Karnaushenko, D.D.; Makarov, D.; Baunack, S.; Schäfer, R.; Schmidt, O.G. Self-Assembled On-Chip-Integrated Giant Magneto-Impedance Sensorics. *Adv. Mater.* **2015**, *27*, 6582–6589. [CrossRef]
161. Thiabgoh, O.; Eggers, T.; Phan, M.-H. A new contactless magneto-LC resonance technology for real-time respiratory motion monitoring. *Sens. Actuators A Phys.* **2017**, *265*, 120–126. [CrossRef]
162. Kobayashi, K.; Iwai, M.; Tanaka, T.; Hata, Y.; Ogata, Y.; Kakinuma, B. Magnetocardiogram measurement using SQUID magnetometer and Magneto-Impedance sensor. *J. Magn. Soc. Jpn.* **2018**, *42*, 61. Available online: <https://www.magnetics.jp/kouenkai/2018/doc/program/06ALL.pdf> (accessed on 2 February 2024).
163. Kurlyandskaya, G.V.; Sanchez, M.L.; Hernando, B.; Prida, V.M.; Gorria, P.; Tejedor, M. Giant-magnetoimpedance-based sensitive element as a model for biosensors. *Appl. Phys. Lett.* **2003**, *82*, 3053–3055. [CrossRef]
164. Kurlyandskaya, G.V. Giant magnetoimpedance for biosensing: Advantages and shortcomings. *J. Magn. Magn. Mater.* **2009**, *321*, 659–662. [CrossRef]
165. Zhu, Y.; Zhang, Q.; Li, X.; Pan, H.L.; Wang, J.T.; Zhao, Z.J. Detection of AFP with an ultra-sensitive giant magnetoimpedance biosensor. *Sens. Actuators B Chem.* **2019**, *293*, 53–58. [CrossRef]
166. Wang, T.; Chen, Y.Y.; Wang, B.C.; He, Y.; Li, H.Y.; Liu, M.; Rao, J.J.; Wu, Z.Z.; Xie, S.R.; Luo, J. A giant magnetoimpedance-based separable-type method for supersensitive detection of 10 magnetic beads at high frequency. *Sens. Actuators A Phys.* **2019**, *300*, 111656. [CrossRef]
167. Blanc-Béguin, F.; Nabily, S.; Gieraltowski, J.; Turzo, A.; Querellou, S.; Salaun, P.Y. Cytotoxicity and GMI bio-sensor detection of maghemite nanoparticles internalized into cells. *J. Magn. Magn. Mater.* **2009**, *321*, 192–197. [CrossRef]
168. Yang, Z.; Liu, Y.; Lei, C.; Sun, X.-C.; Zhou, Y. A flexible giant magnetoimpedance-based biosensor for the determination of the biomarker C-reactive protein. *Microchim. Acta* **2015**, *182*, 2411–2417. [CrossRef]
169. Yang, H.; Chen, L.; Lei, C.; Zhang, J.; Li, D.; Zhou, Z.-M.; Bao, C.-C.; Hu, H.-Y.; Chen, X.; Cui, F.; et al. Giant magnetoimpedance-based microchannel system for quick and parallel genotyping of human papilloma virus type 16/18. *Appl. Phys. Lett.* **2010**, *97*, 043702. [CrossRef]
170. Mahdavi, H.; Rosell-Ferrer, J. In-bed vital signs monitoring system based on unobtrusive magnetic induction method with a concentric planar gradiometer. *Physiol. Meas.* **2017**, *38*, 1226. [CrossRef] [PubMed]
171. Scharfetter, H.; Lackner, H.K.; Rosell, J. Magnetic induction tomography: Hardware for multi-frequency measurements in biological tissues. *Physiol. Meas.* **2001**, *22*, 131. [CrossRef] [PubMed]
172. Ma, L.; Soleimani, M. Magnetic induction tomography methods and applications: A review. *Meas. Sci. Technol.* **2017**, *28*, 072001. [CrossRef]
173. Leontiev, V.S.; Lobekin, V.N.; Saplev, A.F.; Zueva, E.A.; Evasheva, E.E.; Bichurin, M.I. Application of magnetoelectric sensors in biomedicine. *J. Phys. Conf. Ser.* **2021**, *2052*, 012022. [CrossRef]
174. Dong, C.Z.; Liang, X.F.; Gao, J.Y.; Chen, H.H.; He, Y.F.; Wei, Y.Y.; Zaeimbashi, M.; Matyushov, A.; Sun, C.X.; Sun, N.X. Thin Film Magnetoelectric Sensors Toward Biomagnetism: Materials, Devices, and Applications. *Adv. Electron. Mater.* **2022**, *8*, 2200013. [CrossRef]
175. Lobekin, V.N.; Petrov, R.V.; Bichurin, M.I.; Rebinok, A.V.; Sulimanov, R.A. Magnetoelectric sensor for measuring weak magnetic biological fields. *IOP Conf. Ser. Mater. Sci. Eng.* **2018**, *441*, 012035. [CrossRef]
176. Zuo, S.M.; Schmalz, J.; Özden, M.-Ö.; Gerken, M.; Su, J.X.; Niekkel, F.; Lofink, F.; Nazarpour, K.; Heidari, H. Ultrasensitive Magnetoelectric Sensing System for Pico-Tesla MagnetoMyoGraphy. *IEEE Trans. Biomed. Circuits Syst.* **2020**, *14*, 971–984. [CrossRef] [PubMed]
177. Apu, E.H.; Nafiujjaman, M.; Sandeep, S.; Makela, A.V.; Khaleghi, A.; Vainio, S.; Contag, C.H.; Li, J.X.; Balagingham, I.; Kim, T.H.; et al. Biomedical applications of multifunctional magnetoelectric nanoparticles. *Mater. Chem. Front.* **2022**, *6*, 1368–1390.
178. Das, D.; Xu, Z.Y.; Nasrollahpour, M.; Martos-Repath, I.; Zaeimbashi, M.; Khalifa, A.; Mittal, A.; Cash, S.S.; Sun, N.X.; Shrivastava, A.; et al. Circuit-Level Modeling and Simulation of Wireless Sensing and Energy Harvesting With Hybrid Magnetoelectric Antennas for Implantable Neural Devices. *IEEE Open J. Circuits Syst.* **2023**, *4*, 139–155. [CrossRef]

- 
179. Sharma, S.D.; Fischer, R.; Schoennagel, B.P.; Nielsen, P.; Kooijman, H.; Yamamura, J.; Adam, G.; Bannas, P.; Hernando, D.; Reeder, S.B. MRI-based quantitative susceptibility mapping (QSM) and R2\* mapping of liver iron overload: Comparison with SQUID-based biomagnetic liver susceptometry. *Magn. Reson. Med.* **2017**, *78*, 264–270. [[CrossRef](#)]
  180. Li, B.-B.; Ou, L.F.; Lei, Y.C.; Liu, Y.-C. Cavity optomechanical sensing. *Nanophotonics* **2021**, *10*, 2799–2832. [[CrossRef](#)]

**Disclaimer/Publisher’s Note:** The statements, opinions and data contained in all publications are solely those of the individual author(s) and contributor(s) and not of MDPI and/or the editor(s). MDPI and/or the editor(s) disclaim responsibility for any injury to people or property resulting from any ideas, methods, instructions or products referred to in the content.